

Dynamics of transcriptional programs and chromatin accessibility in mouse spermatogonial cells from early postnatal to adult life

Reviewed Preprint

Published from the original preprint after peer review and assessment by eLife.

About eLife's process

Reviewed preprint posted

November 22, 2023 (this version)

Posted to bioRxiv

August 15, 2023

Sent for peer review

August 14, 2023

Irina Lazar-Contes, Deepak K. Tanwar, Rodrigo G. Arzate-Mejia, Leonard C. Steg, Olivier Ulrich Feudjio, Marion Crespo, Pierre-Luc Germain, Isabelle M. Mansuy 

Laboratory of Neuroepigenetics, Brain Research Institute, Medical Faculty of the University of Zurich and Institute for Neuroscience, Department of Health Science and Technology of the ETH Zurich, Zurich, Switzerland • Center for Neuroscience Zurich, ETH and University Zurich • ADLIN Science, Pépinière «Genopole Entreprises», Evry, France

 https://en.wikipedia.org/wiki/Open_access

 Copyright information

Abstract

In mammals, spermatogonial cells (SCs) are undifferentiated male germ cells in testis quiescent until birth that self-renew and differentiate to produce spermatogenic cells and functional sperm across life. The transcriptome of SCs is highly dynamic and timely regulated during postnatal development. We examined if such dynamics involves changes in chromatin organization by profiling the transcriptome and chromatin accessibility in SCs from early postnatal stages to adulthood in mice using RNA-seq and ATAC-seq. By integrating transcriptomic and epigenomic features, we show that SCs undergo massive chromatin remodeling during postnatal development that correlates with distinct gene expression profiles and transcription factors (TF) motif enrichment. We identify genomic regions with significantly different chromatin accessibility in adult SCs that are marked by histone modifications associated with enhancers and promoters. Some of the regions with increased accessibility correspond to transposable element subtypes enriched in multiple TFs motifs and close to differentially expressed genes. Our results underscore the dynamics of chromatin organization in developing germ cells and the involvement of the regulatory genome.

eLife assessment

This study provides **useful** datasets on gene expression and chromatin accessibility profiles in spermatogonial cells at different postnatal ages in mice. Overall, the technical aspects of the sequencing analyses and computational/bioinformatics are **solid**. However, there are concerns with the identity of the isolated cells and the lack of acknowledgment for previous studies that have also performed ATAC-sequencing on spermatogonia of mouse and human testes. The limitations call into question the validity of the interpretations and reduce the potential merit of the findings.

Introduction

Spermatogonial cells (SCs) are the initiators and supporting cellular foundation of spermatogenesis in testis in many species including mammals. In mice, SCs become active one to two days after birth, when they exit mitotic arrest and start dividing to populate the basement membrane of seminiferous tubules. During the first week of postnatal life, a population of SCs continues to proliferate to give rise to undifferentiated A_{single} (A_s), A_{paired} (A_{pr}) and A_{aligned} (A_{al}) cells. The remaining SCs differentiate to form chains of daughter cells that become primary and secondary spermatocytes around postnatal day (PND) 10 to 12. Spermatocytes then undergo meiosis and give rise to haploid spermatids that develop into spermatozoa. Spermatozoa are then released in the lumen of seminiferous tubules and continue to mature in the epididymis until becoming capable of fertilization by PND 42-48 (De Rooij, 2017 [↗](#); Kubota and Brinster, 2018 [↗](#); Oatley and Griswold, 2017 [↗](#)).

Recent work showed that SCs in early postnatal life have distinct transcriptional signatures (Green et al., 2018 [↗](#); Hammoud et al., 2014 [↗](#); Hermann et al., 2018 [↗](#); Law et al., 2019 [↗](#)). During the first week of postnatal development, SCs display unique features necessary for the rapid establishment and expansion of the cell population along the basement membrane. This includes high expression of genes involved in cell cycle regulation, stem cell proliferation, transcription and RNA processing (Grive et al., 2019 [↗](#)). In comparison, genes expressed in adult SCs are involved in the maintenance of a balance between proliferation and differentiation, and help constitute a steady cell population that ensures sperm formation across life. Previous transcriptome analyses have revealed that adult SCs prioritize pathways related to paracrine signaling and niche communication, as well as mitochondrial functions and oxidative phosphorylation (Grive et al., 2019 [↗](#); Hermann et al., 2018 [↗](#)). Epigenetic changes such as histone tail modifications and DNA methylation have also been reported in SCs during postnatal development (Hammoud et al., 2014 [↗](#); Hammoud et al., 2015 [↗](#)). Today however, the relationship between the transcriptome dynamics and chromatin landscape in SCs during the transition from early postnatal to adult stage has not been fully characterized.

We characterized the transcriptome and the profile of chromatin accessibility in SCs during the transition from early postnatal to adult stages. The results reveal extensive changes in transcription and in chromatin accessibility in particular, an increase in chromatin accessibility at enhancer regions in adult SCs compared to postnatal SCs. Regions with changes in chromatin accessibility are enriched in binding motifs of several TFs that are differentially expressed between postnatal and adult stages, suggesting a possible role in changes in chromatin accessibility. Analyses of chromatin accessibility at transposable elements (TEs) identified previously uncharacterized changes at long terminal repeats (LTR) and LINE L1 subtypes between developing and adult SCs. Together, these findings suggest a functional link between transcriptional dynamics and chromatin accessibility in SCs during development, and underscore the plasticity of genome organization in germ cells.

Results

FACS enriches SCs collected from postnatal and adult mouse testis

We collected testes from 8- and 15-day old pups (PND8 and 15) and adult males and prepared cell suspensions from each animal by enzymatic digestion. The preparations were enriched for SCs by fluorescence-activated cell sorting (FACS) using specific surface markers (Kubota et al., 2004 [↗](#)) (Fig. 1A, B [↗](#)). The purity of sorted cells was evaluated by immunocytochemistry using PLZF

(ZBTB16), a well-established marker for undifferentiated SCs (Costoya et al., 2004). FACS enriched cell populations from 3-6% PLZF+ (before FACS) to 85-95% PLZF+ (Fig. 1B), suggesting a high SCs enrichment.

To validate the molecular identity of enriched SCs populations, we profiled their transcriptome at PND8, PND15 and adulthood by total RNA sequencing (RNA-seq) (n=6 for each group) and examined the expression of known spermatogonial stem cell and somatic markers (Leydig and Sertoli cells) (Fig. 1C and Fig. S1A, B). Classical SCs markers such as *c-kit* (Schrans-Stassen et al., 1999), *Id4* (Helsel et al., 2017; Sun et al., 2015), *Lin28a* (Chakraborty et al., 2014; Wang et al., 2020), *Zbtb16* (Costoya et al., 2004; Song et al., 2020) and *Gfra1* (He et al., 2007) were robustly expressed in all SCs samples at each developmental stage (Fig. 1C and Fig. S1A, B), indicating high purity of sorted cells. In contrast, low to negligible expression of somatic cells markers such as *Vim* (Bernardino et al., 2018) and *Tspan17* (Gewiss et al., 2021) for Sertoli cells, and *Fabp3* and *Hsd3b1* for Leydig cells (Sararols et al., 2021) (Fig. 1C) was detected. To further validate the samples purity, we manually curated a list of spermatogonial and somatic cell markers derived from recent single-cell RNA-seq datasets (Cao et al., 2021; Sararols et al., 2021) and determined their expression level in our datasets. Again, we detected robust and consistent expression of all reported spermatogonial markers and low expression of somatic cells markers in all samples at each developmental stage (Fig. S1A). These results confirm the efficiency of our FACS-based enrichment method.

Dynamic transcriptomic states characterize postnatal and adult SCs

We examined the transcriptome dynamics of SCs from postnatal to adult stages by identifying differentially expressed genes (DEGs) in the RNA-seq datasets. We used a stringent cut-off (adjusted- $P \leq 0.05$, abs Log_2 fold change (FC) ≥ 1) on 17,000 genes expressed during at least one developmental stage (See Methods). A total of 663 DEGs were identified between PND8 and PND15 (146 down-regulated and 517 up-regulated) and 2483 DEGs between PND15 and adult stage (914 down-regulated and 1579 up-regulated) (Fig. 1D-E and Table S1). Consistent with previous reports (Hammoud et al., 2015), we observed a dynamic regulation of germ cell factors, transcription factors (TF) involved in core pluripotency pathways and signaling molecules important for self-renewal (Fig. S1B). For instance, *Pou5f1* (*Oct4*), a TF necessary for pluripotency (Nichols et al., 1998), is significantly down-regulated in adult SCs while the TFs *Klf4* and *Sox2*, also needed for pluripotency (An et al., 2019), are expressed similarly in postnatal and adult stages although at different level (i.e *Klf4* is expressed more than *Sox2*) (Fig. S1B).

We conducted Gene Ontology (GO) enrichment analyses to identify the biological processes which DEGs are involved in. GO analyses showed that DEGs between PND8 and PN15 are involved in cell differentiation, cilium movement, sperm motility and transcription and include for instance, TFs such as *Junb*, *Hoxb6*, *Cebpa* and *Pparg* (Fig. 1F and Table S2). Further, genes coding for histone proteins such as histone H2B *Hist2h3b* and epigenetic modifiers like the methyltransferase *Pygo1* and histone acetyl-transferase *Ncoa1* are also differentially expressed between PND8 and 15. Interestingly, genes down- or up-regulated between postnatal stages are involved in different processes. While down-regulated genes are implicated in cell differentiation, cell migration and regulation of proliferation for instance, *Cdkn1a* that is down-regulated at PND15 regulates genetic diversity during spermatogenesis (Kanatsu-Shinohara et al., 2022), up-regulated genes are rather involved in germ cell development, cell signalling, insulin secretion and transcription (Fig. S1C and Table S2). Further, DEGs between PND15 and adulthood have roles in reproduction, spermatogenesis, cell differentiation, DNA replication, glycolysis and extracellular matrix (ECM)-receptor interaction pathways (Fig. 1G, Fig. S1D and Table S2). For example, the DNA methyltransferase *Dnmt1*, necessary for genome regulation (Edwards et al., 2017) and *Col4a2*, a subunit of type IV collagen and component of the basal membrane (Reissig et al., 2019), are specifically down-regulated in adult SCs (Fig. S1C). Interestingly, expression of collagen has been

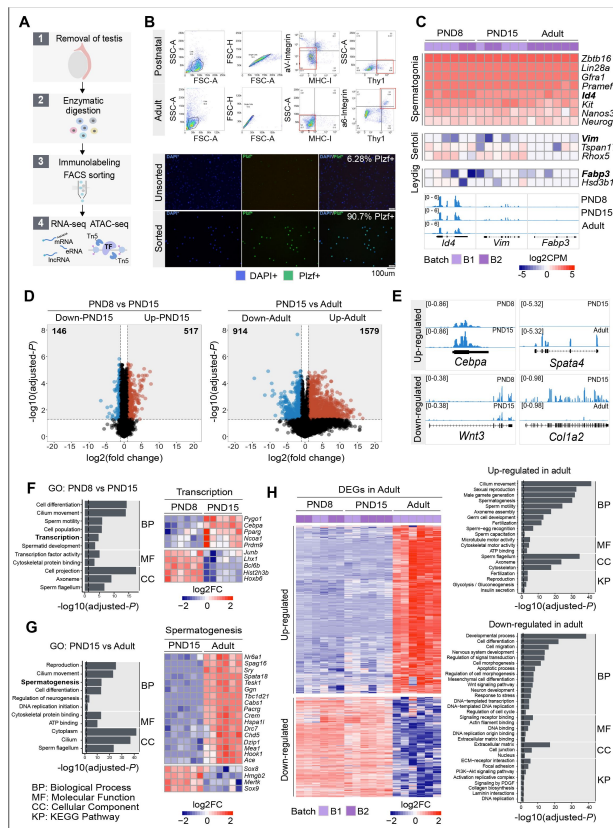


Figure 1.

Transcriptome dynamics between early postnatal and adult SCs.

- (A) Schematic representation of the experimental strategy to isolate and analyse SCs from postnatal or adult male mice.
- (B) Upper panel: Representative dot plots of the sorting strategy for enrichment of postnatal and adult SCs. Gating based on side scatter/forward scatter (SSC-A/FSC-A) and forward scatter (height/forward scatter) (FSC-H/FSC-A) area was conducted to exclude cell debris and clumps. Lower panel: Representative immunocytochemistry on unsorted and sorted PND15 cells with anti-PLZF antibody and DAPI (nuclei) showing enrichment of PLZF+ cells after FACS.
- (C) Heatmap of expression profile of selected markers of SCs and different testicular somatic cells extracted from total RNA-seq data on PND8, PND15 and adult samples (n=6 for each group). Key genes for stem cell potential, stem and progenitor spermatogonia and Leydig and Sertoli cells were chosen to assess the enrichment of SCs in the sorted cell populations. Each row in the heatmap represents a biological replicate from two experimental batches (B1 and B2). At the bottom are shown Integrative Genomics Viewer (IGV) tracks for aggregated RNA-seq signal for PND8, PND15 and adult over key genes used as markers. Gene expression is represented as Log2CPM (counts per million).
- (D) Volcano plot of differentially expressed genes (DEGs) (adjusted- $P \leq 0.05$ and absolute $\text{Log}_2\text{FC} \geq 1$) between PND8 and PND15 (left) and PND15 and adult (right). Figures in grey boxes indicate the number of down- and up-regulated DEGs in each comparison.
- (E) Genomic IGV snapshots of exemplary DEGs showing aggregated RNA-seq signal for PND8, PND15 and adult SCs.
- (F) Left: Bar-plot of GO categories enriched in DEGs between PND8 and PND15 (adjusted- $P \leq 0.05$). Dotted line indicates threshold value for significance of 0.05. Right: Heatmap of DEGs between PND8 and PND15 belonging to the GO category "Transcription". Each row represents a biological replicate from two experimental batches. Shown are Log_2FC with respect to average at PND8.
- (G) Left: Bar-plot of GO categories enriched in DEGs between PND15 and adult (adjusted- $P \leq 0.05$). Dotted line indicates threshold value for significance of 0.05. Right: Heatmap of DEGs between PND8 and PND15 belonging to the GO category "Spermatogenesis". Each row represents a biological replicate from two experimental batches. Shown are Log_2FC with respect to average at PND8.
- (H) Left: Heatmap of all DEGs specific to adult SCs. Each row represents a biological replicate from two experimental batches (B1 and B2). Shown are Log_2FC with respect to average at PND8. Right: Bar-plots of GO categories enriched in up-regulated (adjusted- $P \leq 0.05$) (top) or down-regulated (adjusted- $P \leq 0.05$) (bottom) genes in adult SCs. Dotted line indicates threshold value for significance of adjusted- $P = 0.05$.

associated to a high proliferative potential and the ability to form germ cell colonies in SCs (He et al., 2005 [↗](#)), suggesting that regulation of collagen genes in adult SCs may decrease germ-stem cell potential. Genes up-regulated in adult SCs are involved in cilium movement, germ cell development and glycolysis (Table S2).

We then examined the differences and similarities of transcriptional profiles across the three developmental stages. To identify unique or common changes in gene expression during the transition from early postnatal to adult stages, we compared the list of DEGs at PND8 versus PND15 and at PND15 versus adulthood. Remarkably, the vast majority of DEGs show significant stage-specific changes in transcription (Fig. S2A). For instance, 75% (495/663) of DEGs between PND8 and PND15 are not statistically changed in the transition to adult SCs (Fig. S2B and Table S1 and S2). Similarly, 93% (2325/2493) of DEGs in adult SCs are not statistically changed when compared to PND8 versus PND15 SCs (Fig. 1H [↗](#) and Table S1 and S2). GO enrichment analyses showed that adult-specific down-regulated genes are involved in cell differentiation, cell migration, regulation of signal transduction and Wnt signalling, regulation of DNA replication and transcription as well as collagen biosynthesis and laminin interactions while adult-specific up-regulated genes are involved in sexual reproduction, male gamete generation, germ cell development, cilium movement and glycolysis (Fig. 1H [↗](#) and Table S1 and S2).

Interestingly, a small fraction of all DEGs (4.9%) are detected as significantly changed in the same direction and magnitude (adjusted- $P \leq 0.05$, $\text{absLog}_2\text{FC} \geq 1$) across the three developmental stages (Fig. S2C and Table S1 and S2). For instance, 121 genes are consistently up-regulated from PND8 to adult stage, while just 26 are consistently down-regulated from PND8 to adult stage (Fig. S2C). Such DEGs are involved in different biological pathways like chromatin organization (Table S2). In particular, the histone gene clusters displayed significant down-regulation across postnatal development and in adulthood (Table S2).

Landscape of chromatin accessibility in SCs during postnatal development

Cellular differentiation is generally accompanied by changes in chromatin accessibility at regulatory elements (Atlasi et al., 2017). We examined how chromatin accessibility in SCs is modified during development using omni-ATAC-seq (Corces et al., 2017 [↗](#)). We focused on SCs at PND15 and adulthood, stages that showed the highest changes in gene expression (Fig. 1 [↗](#)). Accessible regions were identified by peak-calling on merged nucleosome-free fragments (NFF) as proxy for genomic regions with potential regulatory activity. We identified 158,977 peaks with clear ATAC-seq signal compared with surrounding genomic regions (Fig. S3A and Table S3). Most accessible regions were located at distal intergenic regions (38%), introns (28%) and putative promoter regions (23%) (Fig. S3B, C) and encompassed sequences enriched for histone PTMs associated with active chromatin such as H3K4 mono-, di- and tri-methylation (Fig. S2D). Notably, signal enrichment was higher for H3K4 methylation than for other histone PTMs (Fig. S3D). These results are consistent with previous observations that ATAC-seq peaks are identified at regulatory elements such as enhancers and promoters and are preferentially located at genomic regions with nucleosomes carrying H3K4me (Henikoff et al., 2020 [↗](#)).

We then examined differences in chromatin accessibility between PND15 and adult SCs by differential accessibility analysis. 3212 differentially accessible regions (DARs) were identified (adjusted- $P \leq 0.05$, $\text{absLog}_2\text{FC} \geq 1$) with a total of 760 regions with decreased chromatin accessibility (DARs-down) and 2452 regions with increased accessibility (DARs-up) in adult SCs (Figure 2A [↗](#), B and Table S3). DARs were predominantly localized in distal intergenic regions (54% DARs-down, 37% DARs-up) and introns (33% DARs-down, 36% DARs-up) with a minority located in putative promoter regions (8% DARs-down, 12% DARs-up), consistent with the genomic distribution of all

detected ATAC-seq peaks (**Fig. 2C**). GO analyses of the closest genes assigned to each DAR showed that these genes are involved in male gonad development, cell adhesion, sex differentiation and regulation of cell communication among others (**Fig. 2D, E**).

Epigenomic annotation of DARs using high-quality publicly available ChIP-seq datasets for postnatal SCs (Cheng et al., 2020) revealed that DARs are predominantly located in regions enriched for histone PTMs associated with enhancers and promoters. 51% of regions with increased accessibility are located at genomic loci that carry histone PTMs since early postnatal stages, and about half (48%) overlap with regions significantly enriched in H3K4me1, a histone PTM associated to enhancers. In contrast, 80% of regions with decreased accessibility are located in regions with H3K4me1 and 1/3 (33%) also overlap with the repressive histone PTM, H3K27me3 (**Fig. 2F**). Interestingly, while 16% of regions with increased accessibility are located at potential active regulatory elements that carry H3K27ac, none of the regions with decreased accessibility overlap with H3K27ac (**Fig. 2F**). Therefore, our data indicate that the transition from postnatal to adult SCs is accompanied by discrete, yet robust, changes in chromatin accessibility at potential regulatory elements, suggesting their involvement in the control of gene transcription.

DARs are associated with binding sites for distinct families of TFs

We examined the relationship between differences in chromatin accessibility and TF binding by TF motif analysis using DARs as input. We observed that regions with decreased accessibility in adult SCs are enriched for binding motifs of members of specific TF families such as KLF (KLF2, KLF5, KLF11, KLF12, KLF15, KLF16), SP (SP1-5, SP9), FOXO (FOXO1, FOXO3), ETS (ETV1-6) among others (**Fig. 3A** and

Table S4). Expression analyses showed that many of these TFs are differentially expressed in postnatal or adult SCs (adjusted- $P < 0.05$, 10 down-regulated and 11 up-regulated) (**Fig. 3B, C**). For example, KLF11,12 and 15, TFs that regulate stem cell maintenance and development (Bialkowska et al., 2017), are upregulated in adult SCs compared to PND15 (**Fig. 3C**). These TFs and their motif match top enriched motifs detected in DARs in adult SCs (**Fig. 3A**). The SP family of TFs also show differential expression and enrichment of binding motifs in regions with decreased accessibility. SP5, which has its lowest expression in adult SCs (**Fig. 3B, C**), promotes self-renewal of mESCs by directly regulating *Nanog* (Tang et al., 2017).

Members of the FOXO family of TFs also have an enrichment of motifs in regions with decreased accessibility. While FOXO3 has increased expression from PND15 onwards, FOXO1 is decreased in adult compared to postnatal SCs (**Fig. 3B, C**). Interestingly, FOXO1 and FOXO3 regulate spermatogonial stem cell function and maintenance in mouse (Goertz et al., 2011). Finally, ETS-type of TFs also show differential expression during SCs development and their motif is enriched in regions with decreased accessibility. ELK4 is up-regulated in adult SCs and can act as a transcriptional repressor via recruitment of the HDAC Sirt7 and deacetylation of H3K18ac (**Fig. 3B-D**) (Barber et al., 2012). ELK4 can also act as transcriptional activator of immediate early genes such as *c-Fos* (Dalton and Treisman, 1992). Interestingly, *c-Fos* itself codes for a TF important for the regulation of proliferation (He et al., 2008) and shows a trend towards up-regulation in adult SCs (Table S1). In contrast, GABPA is downregulated in adult SCs compared to PND15, and has been involved in the regulation of proliferation in mESCs (Ueda et al., 2017).

Regions with decreased chromatin accessibility also show an enrichment for the binding motif of the TF DMRT1. *Dmrt1* is progressively repressed during SCs postnatal development and is the lowest in adult SCs (**Fig 3B, C and E**). DMRT1 can act either as a repressor or activator and controls testis development and male germ cell proliferation (Zhang et al., 2016). DMRT1 can inhibit meiosis and promote mitosis in SCs by repressing *Stra8* (Matson et al., 2010). Consistently, we observed transcriptional repression of *Stra8* in adult SCs (Table S1).

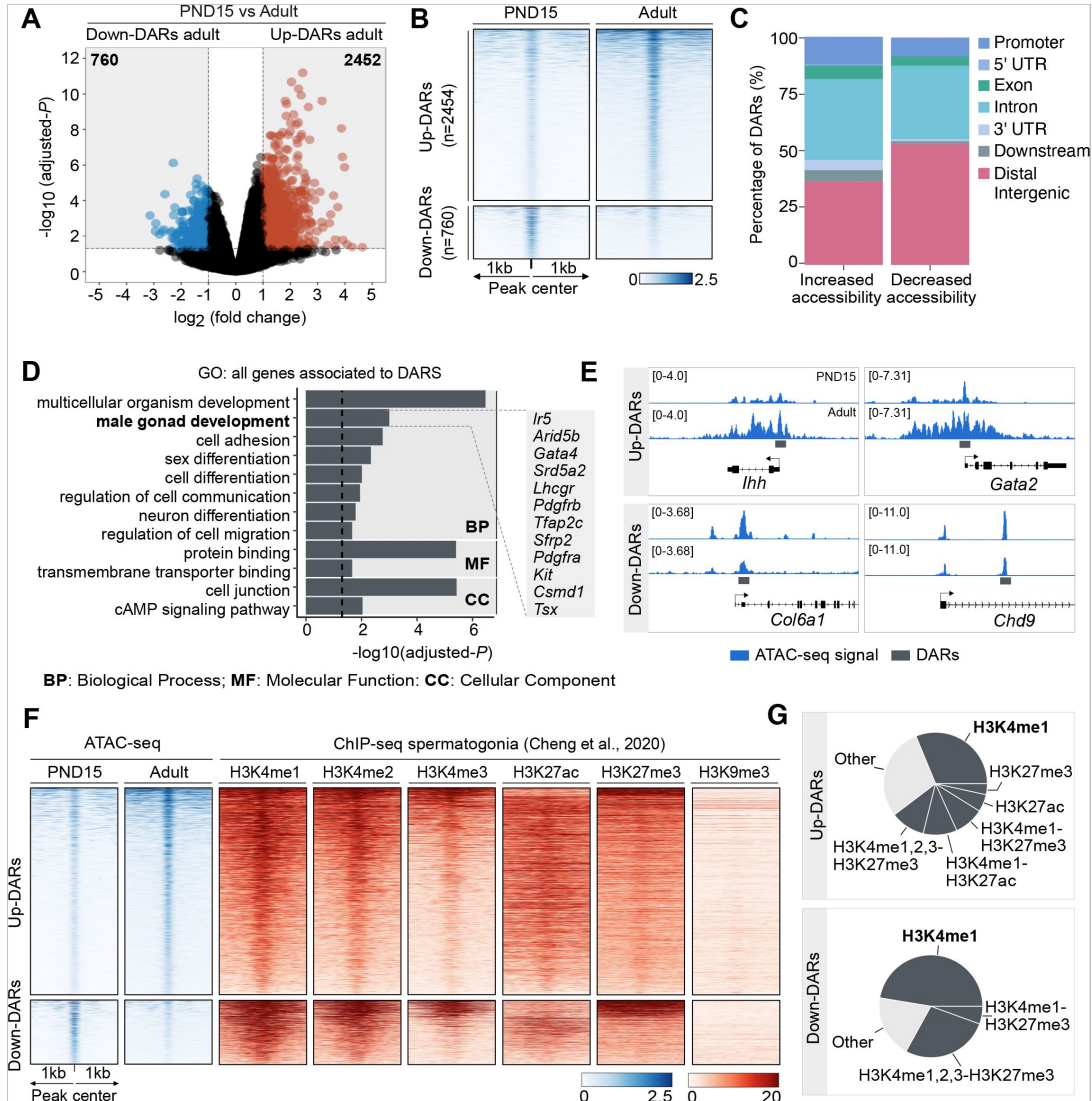


Figure 2.

Dynamics of chromatin accessibility of SCs during the transition from postnatal to adult stage

(A) Volcano plot of DARs obtained by ATAC-seq (adjusted- $P \leq 0.05$ and absolute $\text{Log}_2\text{FC} \geq 1$) between PND15 and adult SCs. Figures in grey boxes indicate the number of DARs with decreased (Down) or increased (Up) chromatin accessibility in PND15 compared to adult SCs.

(B) Heatmaps showing normalized ATAC-seq signal for all identified DARs comparing PND15 and adult stages. Each row represents a 2kb genomic region extended 1kb down- and upstream from the centre of each identified DAR (as shown in A). Rows are ordered in a decreasing level of mean accessibility.

(C) Bar plot illustrating the genomic distribution of DARs between PND15 and adult SCs.

(D) Bar plot of GO categories for associated genes assigned by proximity to all DARS. Dotted line indicates threshold value for significance of adjusted- $P = 0.05$.

(E) IGV tracks for ATAC-seq signal for PND15 and adult SCs showing DARS (red box) located at promoters and intergenic regions.

(F) Heatmaps showing normalized ChIP-seq signal for different histone marks in adult SCs (public data derived from Cheng et al., 2020) at all identified ATAC-seq peaks from PND15 and adult stages. Each row in the heatmap represents a 2kb genomic region extended 1kb down- and up-stream from the centre of each identified peak. Shown data correspond to non-regenerative SCs as stated in Cheng et al., 2020.

(G) Pie charts showing the overlap of all identified DARS with genomic regions significantly enriched for different histone marks in adult SCs (public data derived from Cheng et al., 2020).

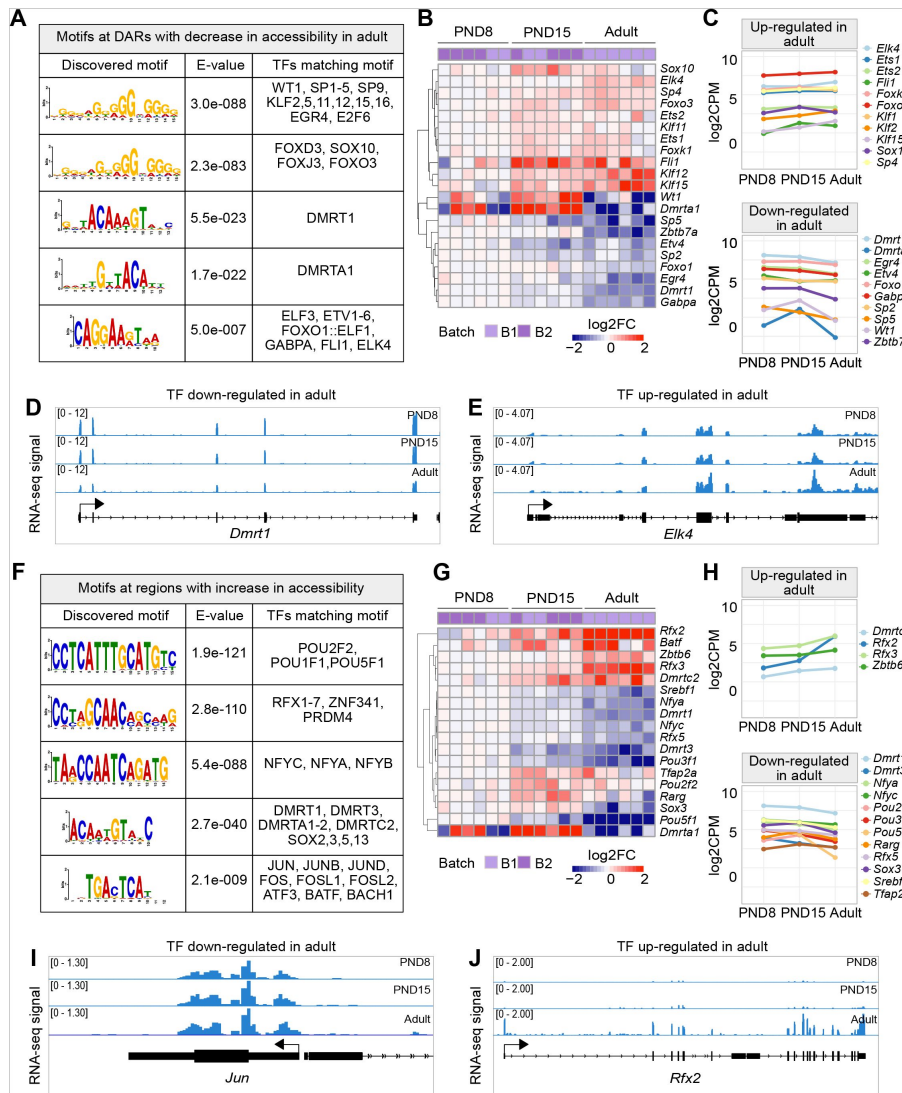


Figure 3.

TF binding motifs at DARs and their transcriptional dynamics during the transition from postnatal to adult SCs

(A) Table of top five enriched motifs in genomic regions with decrease in chromatin accessibility in adult SCs and TF matching motifs. A full list of TF motifs is provided in Table S4.

(B) Heatmap of expression profile of TFs with motifs in genomic regions with decreased chromatin accessibility shown in (A). Each row represents a biological replicate from two experimental batches. Unsupervised hierarchical clustering was applied to each row and a dendrogram indicating similarity of expression profiles among genes is shown. Shown are Log₂FC with respect to average of PND8 SCs.

(C) Line-plots of average expression of each gene displayed in the heatmap in (B) showing the dynamics of gene expression across PND8, PND15 and adult SCs.

(D, E) Genomic snapshot from IGV showing aggregated RNA-seq signal from PND8, PND15 and adult SCs for the TFs D) *Dmrt1* and E) *Elk4*.

(F) Table of top five enriched motifs in genomic regions with increase in chromatin accessibility in adult SCs and TF matching motifs. A full list of TF motifs is provided in Table S4.

(G) Heatmap of expression profile of TFs with motifs in genomic regions with increase in chromatin accessibility shown in (F). Shown are Log₂FC with respect to the average of PND8 SCs.

(H) Line-plots of average expression of each gene displayed in the heatmap in (G) showing the dynamics of gene expression across SCs development.

(I, J) Genomic snapshot from IGV showing the aggregated RNA-seq signal from PND8, PND15 and adult SCs for the TFs I) *Jun* and J) *Rfx2*.

Next, we identified motifs overrepresented in regions with increased chromatin accessibility in adult SCs. The identified motifs correspond to binding motifs of members of specific TF families such as POU (POU2F2, POU1F1, POU5F1), RFX (RFX1-7), DMRT (DMRT1, DMRT3, DMRTA1-2, DMRTC2), SOX (SOX2, SOX3, SOX5, SOX13), NFY (NFYA, NFYB, NFYC) and AP-1 (JUN, JUNB, JUND, FOS, ATF3, BATF) (Fig. 3F and Table S4). A subset of them is also differentially expressed (adjusted- $P < 0.05$, 13 down-regulated and 5 up-regulated). The most overrepresented motif is similar to the binding motif of the POU family of TFs, which are critical regulators of stem cells (Nichols et al., 1998). *Pou1f1* and *Pou5f1* are transcriptionally repressed in adult SCs while *Pou2f2* is maximally expressed in PND15 SCs and down-regulated in adult cells (Fig. 3G, H). We also identified motifs for members of the RFX family of TFs, which are master regulators of ciliogenesis (Choksi et al., 2014) implicated in regulation of neural stem cells (Kawase et al., 2014). RFX2 is robustly expressed in adult SCs (Fig. 3G, H and I) and has been reported to induce the expression of ciliary genes in association with the TF FOXJ, which has a trend towards up-regulation in adult SCs (Fig. S4) (Quigley and Kintner, 2017). Interestingly, ciliary genes are among the top genes specifically up-regulated in adult SCs (Fig. 1H), suggesting a regulatory relationship between RFX2 and ciliary genes expression in adult SCs.

Other binding motifs enriched at regions with increased accessibility correspond to members of the NF-Y complex, NF-YA, NF-YB and NF-YC. In mESCs, NF-Y TFs facilitate a permissive chromatin conformation and play an important role in the expression of core ESC pluripotency genes (Oldfield et al., 2014). NF-YA/B motif enrichment has also been found in regions of open chromatin in human SCs (Guo et al., 2017). Interestingly, the expression of NF-YA and NF-YC is progressively down-regulated starting at PND15 (Fig. 3G, H). We also detected an enrichment for the binding motifs of members of the AP-1 family of TFs, which are involved in many processes, from regulation of cell proliferation to differentiation and acute responses to environmental clues (Bejjani et al., 2019; Vierbuchen et al., 2017). Interestingly, except for *Fosl2*, other TFs do not show any significant change in transcription in postnatal or adult SCs and are either constitutively expressed or repressed. For instance, c-FOS and JUN are robustly expressed in postnatal and adult SCs (Fig. 3J) consistent with their role in promoting the proliferative potential of spermatogonial stem cells (He et al., 2008; Wang et al., 2018). Together, these data reveal that a shift in TFs repertoire accompanies chromatin reorganization occurring in SCs during postnatal to adult development.

A subset of DARs is associated with differential gene expression

Thus far, our results show that in SCs, the transition from postnatal to the adult stages is accompanied by changes in gene expression and chromatin accessibility. In some instances, differences in gene expression can be correlated with differences in chromatin accessibility of regulatory elements. Since DARs in postnatal and adult SCs overlap with putative enhancer and promoter elements, we examined if these changes in chromatin accessibility correlate with changes in gene expression. First, we tested if promoter regions of DEGs (± 2.5 kb from TSS) have differential chromatin accessibility by identifying all possible ATAC-seq peaks located in promoters and calculating an average accessibility signal. No significant difference was detected for down-regulated genes in adult SCs, despite a trend for decreased accessibility around the TSS (Fig. 4A). However, down-regulated genes had a significant increase in chromatin accessibility in their body (Fig. 4B). Up-regulated genes had a significant increase in chromatin accessibility both at the promoter region and gene body (Fig. 4A, B). Then, we conducted motif enrichment analyses and identified families of TFs with overrepresented binding motifs at the promoter of DEGs. Binding motifs for members of KLF and SP family of TFs were overrepresented in the promoter of both down- and up-regulated DEGs, while motifs for members of TF families SOX and NFY were detected only in the promoter of down-regulated genes. Promoters of up-regulated genes were specifically enriched in motifs for RFX and AP-1 (Fig. 4C). These observations suggest that changes in chromatin accessibility, in particular at the promoter of up-regulated DEGs may be associated with differential binding of RFX and AP-1 TFs.

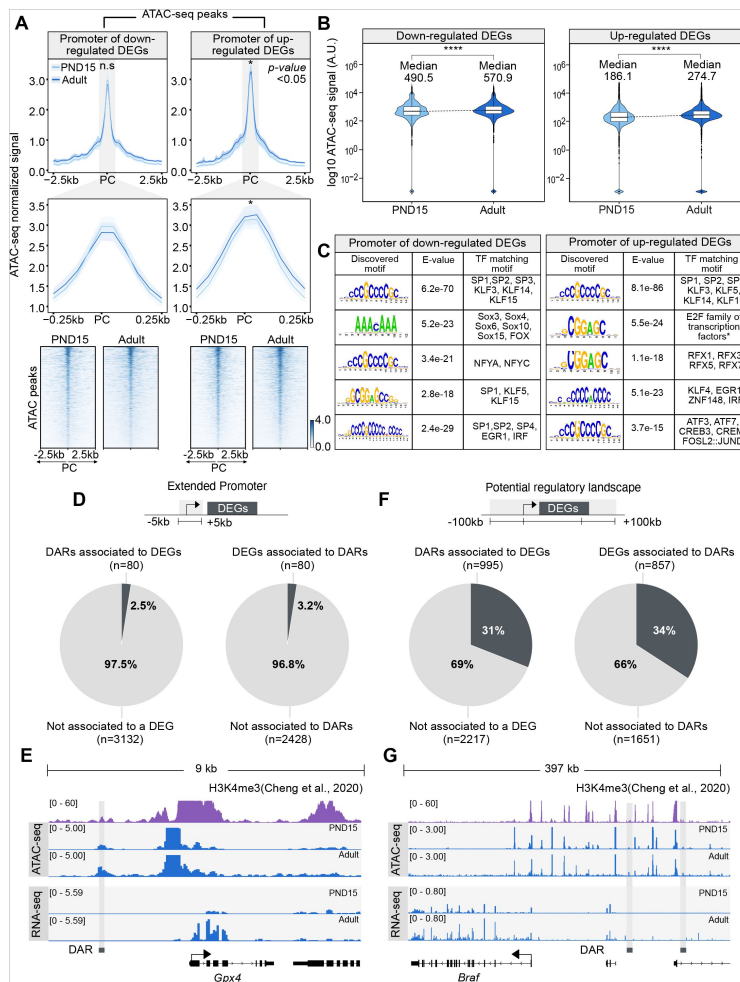


Figure 4.

Chromatin accessibility dynamics at DEGs during the transition from postnatal to adult SCs

(A) *Top*, profile plots of ATAC-seq signal from PND15 and adult SCs over all ATAC-seq peaks located within a genomic region of 5kb surrounding the TSS of DEGs. Mean (line) and bootstrap confidence interval (area, shadow lines) computed over all non-overlapping 50bp genomic regions. n.s., non-significant differences at TSS region. *, significant difference in signal between PND15 and adult at p -value < 0.05. PC, peak center from ATAC-seq data. Profile plots for all ATAC-seq peaks surrounding the TSS of down-regulated (top left) or up-regulated (top right) DEGs. *Middle*, profile plots of ATAC-seq signal from PND15 and adult SCs over all ATAC-seq peaks located within a genomic region of 500bp surrounding the TSS of DEGs. *Bottom*, heatmaps showing normalized ATAC-seq signal from PND15 and adult for all ATAC-seq peaks surrounding the TSS of all down-regulated (left) or up-regulated (right) DEGs. Each row in the heatmap represents a 2kb genomic region extended 1kb down- and up-stream from the center of each identified peak. Row Are ordered in a decreasing level of mean accessibility taking PND15 as reference.

(B) Violin plots of average ATAC-seq signal for PND15 and adult SCs over gene body of down-regulated (left) or up-regulated (right) DEGs. **** p < 0.0001.

(C) TF motif enrichment analysis for all ATAC-seq peaks surrounding the TSS of all down-regulated (left) or up-regulated (right) DEGs.

(D) *Left*, pie chart of percentage of DARs overlapping the extended promoter of DEGs (+/- 5kb from TSS). *Right*, pie chart of percentage of DEGs associated with a DAR.

(E) IGV tracks for an example of DAR associated to the extended promoter (+/- 5kb from TSS) of a DEG. Shown are tracks for RNA-seq and ATAC-seq signal for PND15 and adult SCs generated in this study and signal track for H3K4me3 from SCs derived from public ChIP-seq data (Cheng et al., 2020).

(F) *Left*, pie chart of percentage of DARs overlapping potential regulatory sequences of DEGs (+/-100kb from start and end of gene). *Right*, pie chart of the percentage of DEGs associated with a DAR.

(G) IGV tracks for an example of DAR associated with potential regulatory sequences (+/-100kb from start and end of gene) of a DEG.

Next, we examined the overlap between DARs and the promoter of DEGs. Unexpectedly, only 3.2% of all promoters of DEGs overlap with at least one DAR (Fig. 4D). The majority of overlapping DARs (71%) is associated with promoters of up-regulated genes in adult SCs (Fig. 4D). For example, *Gpx4*, a peroxidase involved in the control of stemness (Hu et al., 2021), is transcriptionally active in adult SCs and has an open chromatin at its promoter region (Fig. 4E). Since the majority of DARs are located at distal intergenic regions and have histone PTMs associated with active regulatory elements, we extended our search of their target genes by assigning a large region (+/-100kb) around each DEG. We observed that a third of DEGs were associated with at least one DAR (Fig. 4F), with the majority of DARs (69%) overlapping regulatory elements of up-regulated genes. For instance, *Braf* is transcriptionally up-regulated in adult SCs, which correlates with increased chromatin accessibility at distal regulatory elements (Fig. 4G). Our results overall show that only a fraction of DEGs is associated with DARs, suggesting that changes in gene expression are not always mirrored at the level of chromatin accessibility, consistent with recent observations (Kiani et al., 2022).

Chromatin accessibility at transposable elements (TEs) undergoes remodeling during the transition from early postnatal to adulthood in SCs

TEs are tightly regulated in the germline by coordinated epigenetic mechanisms involving DNA methylation, chromatin silencing and PIWI proteins-piRNA pathway (Deniz et al., 2019). SCs were recently shown to have a unique landscape of chromatin accessibility at long-terminal repeats (LTRs) retrotransposons, compared with other stages of germ cells in testis (Sakashita et al., 2020). We examined chromatin accessibility at TEs in PND15 and adult SCs by quantifying ATAC-seq reads overlapping TEs defined by UCSC RepeatMasker then analyzing differential accessibility at subtypes level (see Methods section). These analyses showed that SCs transitioning from PND15 to adult stages have significantly different chromatin accessibility at 135 TE subtypes (adjusted- $P \leq 0.05$, $absLog_2FC \geq 1$) (Fig. 5A, B and Table S5). Most TE subtypes have decreased chromatin accessibility (93/135, 68.9%) (Fig. 5A) and 42 have increased accessibility (Fig. 5B) in adult SCs. Differentially accessible TE loci are predominantly located in intergenic (68%) and intronic (25%) regions and 6% re close to a gene (+/-1kb from TSS) (Fig. 5C).

LTR retrotransposons were the most abundant TEs with altered chromatin accessibility, specifically ERVK and ERV1 subtypes (Fig. 5A, B). Exemplary ERVK subtypes with less accessible chromatin included RLTR17, RLTR9A3, RLTR12B and RMER17B (Table S5). Enrichment of RLTR17 and RLTR9 repeats was previously reported in mESCs, specifically at TFs important for pluripotency maintenance such as *Oct4* and *Nanog* (Fort et al., 2014). Interestingly, we identified the promoter region of the long non-coding RNA (lncRNA) *Lncenc1*, an important regulator of pluripotency in mESCs (Fort et al., 2014; Sun et al., 2018), to harbor several LTR loci with decreased accessibility in adult SCs. One of these loci, RLTR17, overlap with the TSS of *Lncenc1*, and its decreased accessibility correlates with markedly lower *Lncenc1* expression in adult SCs (Fig. 5D). *Lncenc1* (also known as *Platr18*) is part of the pluripotency-associated transcript (*Platr*) family of lncRNAs recently identified as potential regulators of pluripotency-associated genes *Oct4*, *Nanog* and

Zfp42 in mESCs (Bergmann et al., 2015). We also identified several other *Platr* genes such as *Platr27* and *Platr14*, whose TSS overlap with LTRs with reduced accessibility, RLTR17 and RLTR16B_MM, respectively (Fig. 5D and Table S5). These two pluripotency-associated transcripts tended to be downregulated in adult SCs but were unchanged at PND8 and PND15 (Fig. 5D and Table S1). The other LTR subtypes with decreased accessibility in adult SCs belong to ERV1, ERVL and MaLR families (Fig. 5A). A few non-LTR TEs also had decreased chromatin accessibility particularly 7 DNA element subtypes, 2 satellite subtypes and 1 LINE subtype, respectively (Table S5).

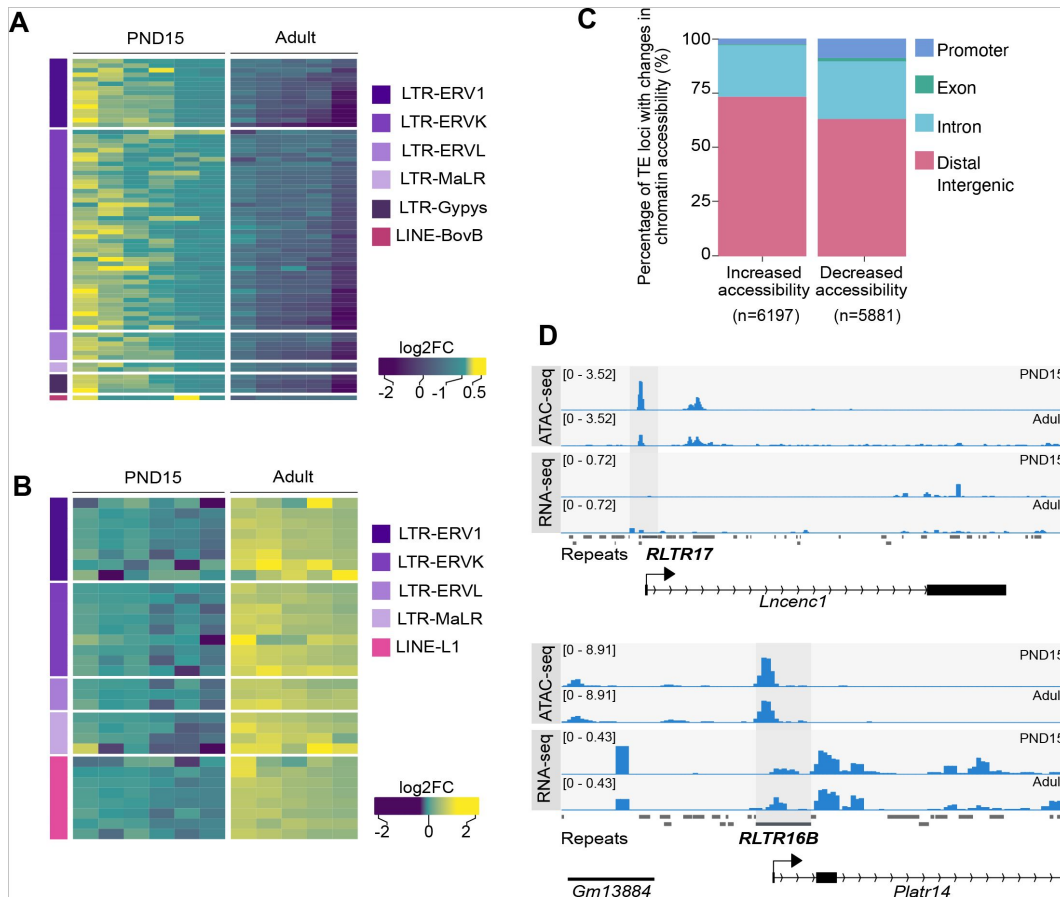


Figure 5.

Differential chromatin accessibility at TEs in PND15 and adult SCs.

(A) Heatmap of LTR and LINE subtypes with decreased accessibility between PND15 and adult SCs extracted from Omni-ATAC data (adjusted $P \leq 0.05$ and $\text{Log}_2\text{FC} \geq 0.5$)

(B) Heatmap of LTR and LINE subtypes with increased accessibility between PND15 and adult SCs extracted from Omni-ATAC data (adjusted $P \leq 0.05$ and $\text{Log}_2\text{FC} \geq 0.5$). Expression changes of these subtypes between adult and PND15 SCs RNA-seq from literature are represented as Log_2FC .

(C) Bar plot illustrating the genomic distribution of DARs between PND15 and adult SCs.

(D) Genomic snapshot from IVG showing aggregated ATAC-seq and RNA-seq signal from PND8, PND15 and adult SCs for *Lncenc1* and *Platr14*. Below signal tracks is shown the RepeatMasker track for the mouse genome, and TEs with changes in chromatin accessibility are highlighted.

TE subtypes with increased accessibility mostly included members of ERVK, ERVL and ERV1 families (24/42, 57.1%) (Table S5). Interestingly, many LINE L1 subtypes had increased chromatin accessibility in adult SCs (Table S5). When parsing the data for more accessible loci within L1 subtypes, we found several L1 loci situated less than +/-5kb from the TSS of olfactory (*Olf*) genes, particularly *Olf* gene clusters on chromosome 2, 7 and 11 (Table S5).

TEs are known to provide tissue-specific substrates for TF binding (Sundaram and Wysocka, 2020). We examined the regulatory potential of differentially accessible LTR subtypes by determining the enrichment of TF motifs in these regions. We grouped LTR subtypes by family (EVK, ERV1, ERVL and ERVL-MaLR families) and observed that among families with less accessible chromatin, ERVKs had the highest number of enriched TF motifs in adult SCs (Table S5). Top hits included TFs with known regulatory functions in cell proliferation and differentiation such as FOXL1 and FOXQ1, stem cell maintenance factors ELF1, EBF1 and THAP11 and TFs important for spermatogenesis PBX3, ZNF143 and NFYA/B (Table S5). ERVLs displayed motif enrichment for very few TFs, among which ETV2, recently reported to be the spermatogonial stem cell factor ZBTB7A and the testis-specific CTCF paralog CTCFL (Table S5) (Green et al., 2018).

More accessible LINE L1 subtypes were highly enriched in TF motifs, particularly in multiple members of ETS, E2F and FOX families (Table S5). The most significant motifs belonged to spermatogonial stem cell maintenance and stem cell potential regulators FOXO1 and ZEB1, as well as TFs recently associated with active enhancers of the stem cell-enriched population of SCs such as ZBTB17 and KLF5 (Table S5) (Cheng et al., 2020). More accessible ERV1s were also enriched in several TF binding sites, including spermatogenesis-related TFs (PBX3, PRDM1, NFYA/B), hypoxia inducible HIF1A and cytokine regulators STAT5A/B, suggesting different metabolic demand between postnatal and adult stage (Table S5).

Discussion

This study examines the transcriptomic landscape and chromatin accessibility of mouse SCs from early postnatal development to adulthood. Using FACS-enriched SCs populations at PND8, PND15 and adulthood, it shows that the transcriptome of SCs is dynamically regulated during development and that many factors including pluripotency-related TFs and signaling molecules are differentially expressed. This correlates with changes in chromatin accessibility although not all DEGs have altered accessibility. TEs such as LTR retrotransposons have modified chromatin accessibility, which in some cases affects pluripotency-associated lncRNAs. TF motif enrichment in differentially accessible TEs suggested various regulatory roles in SCs.

Different transcriptional states characterize the postnatal development of SCs

SCs are known to undergo genome-wide transcriptional changes during development (Grive et al., 2019; Hammoud et al., 2015; Hermann et al., 2018). The present data complement previous findings by showing that postnatal maturation of SCs is accompanied by an overall decrease in the expression of pluripotency markers and differential expression of signaling molecules and regulators of cell cycle and spermatogenesis. The high quality and depth of our RNA-seq datasets allowed us to uncover specific transitional states of SCs postnatal maturation that were not known before. For instance, we observed that while the transition from early to mid-postnatal stages (PND8 to PND15) is accompanied by changes in gene expression, the transition from mid-postnatal to adult stages is more extensive, both in number of regulated genes and magnitude of changes. We also observed a clear trend towards up-regulation of gene expression as postnatal maturation proceeds, that may reflect gradual transcriptional increase for some genes and possibly sharp changes at certain developmental stages for others.

Consistently, many transcriptional regulators and chromatin modifiers are differentially regulated during SCs development. Different families of TFs including factors with a specific role in SCs like RFX and DMRT, and factors with more widespread functions across cell types such as members of the AP-1 family are modulated, suggesting the contribution of multiple classes of TFs to SCs development. Notably, several transcriptional repressors and epigenetic silencers are differentially down-regulated which may explain the marked trend towards transcriptional up-regulation in our datasets (Fig. 1D). Interestingly, we also observed a global down-regulation of histone genes starting at PND15 (Table S1), which may modify the composition and structure of chromatin and be associated with chromatin openness (Prado et al., 2017). Overall, our transcriptional data highlight the yet unappreciated dynamic regulation of TFs and epigenetic/chromatin modifiers in SCs during postnatal development.

Chromatin accessibility in SCs is modified at enhancers during postnatal development

Our results suggest that the transition of SCs from early postnatal to adult life is accompanied by changes in chromatin accessibility. In particular, accessibility is increased in regions enriched in H3K4me1, a histone PTM typically associated with primed enhancers, but also to a lesser extent, in regions enriched in H3K27ac, a mark associated with active regulatory elements (Gasperini et al., 2020; Shlyueva et al., 2014). This suggests that the transition of SCs from postnatal to adult stages involves changes in the regulatory genome, in particular at primed enhancers. Enhancer priming has recently been proposed as an important mechanism for SCs differentiation (McCarrey, 2023). Differences in chromatin accessibility may be partially explained by differential binding of TFs to regulatory elements (Klemm et al., 2019). This may involve at least three non-mutually exclusive events: 1) a change in the abundance of TFs, 2) a change in the epigenetic status of TF binding sites due to different amount and/or activity of epigenetic modifiers, and 3) a change in nucleosome positioning around TF binding sites due to different amount and/or activity of chromatin remodelers. For instance, CpG methylation and nucleosome positioning can influence TF binding at regulatory elements and affect chromatin accessibility (Barisic et al., 2019; Kaluscha et al., 2022). The fact that *Dnmt1* is downregulated in adult SCs concomitantly with differential expression of TFs and chromatin modifiers may explain changes in chromatin accessibility at potential enhancers.

Modest correspondence between transcription and chromatin accessibility in SCs

Despite robust changes in gene expression in adult SCs, only a subset of DARs could be assigned to DEGs. This suggests that transcriptional regulation and chromatin accessibility at regulatory elements are not always linked and can be dissociated, as previously reported (Chereji et al., 2019; Kiani et al., 2022). This implies that chromatin accessibility may be modified without any effects on transcription and conversely, transcription can be activated or repressed without requiring any change in chromatin accessibility. In turn, it is possible that a repressor can be exchanged with an activator at a regulatory element but have no detectable consequences. It is also possible that changes in chromatin accessibility have no immediate effects on transcription but reflect an intermediate state that primes a gene or genomic locus for later activation or repression such as observed with developmentally- or experience-dependent primed enhancers (Marco et al., 2020; Rada-Iglesias et al., 2011). Consistently, the majority of DARs with increased accessibility overlap with regions enriched in H3K4me1, a histone PTM characteristic of primed enhancers thought to control future transcriptional responses in different cell types (Rada-Iglesias et al., 2011). These regions may be important for responses to external cues in adult SCs. The apparent lack of correspondence between transcription and accessibility may also be technical and due to the stringency of filters we used to assign genomic loci to DARs. We cannot exclude the possibility that modest changes in accessibility ($<\log_2FC1$) correspond to changes in TF occupancy. Chromatin accessibility has been suggested to not be the primary determinant of chromatin-mediated gene

regulation (Chereji et al., 2019). Such possibility could be addressed by examining genome-wide maps of TFs, cofactors and RNA-Pol II occupancy that would provide more accurate information about the regulatory genome and its relationship with observed gene expression programs.

Chromatin accessibility at TEs during SCs maturation

Our results reveal differences in chromatin accessibility and TFs motif landscape at different TEs subtypes between PND15 and adult SCs. ERVK and ERV1 subtypes were the most abundant categories of TEs that become less accessible in adult SCs, whilst LINE L1 subtypes gained accessibility. Although the majority of these TEs reside in intergenic and intronic regions, we could detect specific loci belonging to differentially accessible ERVK and LINE L1 subtypes localized nearby TSS of distinct gene families. Notably, ERVKs are known to play an important role in the regulation of mRNA and lncRNAs transcription during spermatogenesis (Davis et al., 2017; Sakashita et al., 2020 [↗](#)). The landscape of chromatin accessibility at LTRs loci in SCs is known to be unique compared to other mitotic germ cells and meiotic gametes in testis (Sakashita et al., 2020 [↗](#)).

RLTR17, one of the LTR subtypes with decreased chromatin accessibility in adult SCs overlaps with the TSS of several downregulated lncRNAs from the *Platr* family. *Platr* genes, including *Lncenc1* and *Platr14* identified in our study, are LTR-associated lncRNAs important for gene expression programs in ESCs (Bergmann et al., 2015 [↗](#)). Interestingly, RLTR17 has also previously been linked to pluripotency maintenance. In mESCs, it is highly expressed and enriched in open chromatin regions and has been shown to provide binding sites for the pluripotency factors Oct4 and Nanog (Fort et al., 2014 [↗](#)). Therefore, we suggest that RLTR17 chromatin organization may play a role in regulating pluripotency programs between early postnatal and adult SCs.

In contrast to decreased accessibility at LTRs loci, LINE L1 subtype had increased accessibility in adult SCs. Some of these L1 loci were located close to olfactory receptor genes with upregulated mRNA expression. Recent findings in mouse and human ESCs suggest a non-random genomic localization of L1 elements, specifically at genes encoding proteins with specialized functions (Lu et al., 2020 [↗](#)). Among them, the *Olfir* gene family was the most enriched in L1 elements (Lu et al., 2020 [↗](#)). Although their role in SCs is currently not established, *Olfir* proteins have been implicated in swimming behaviour of sperm cells (Fukuda and Touhara, 2005 [↗](#)). Given their dynamic regulation in SCs, we speculate that *Olfir* genes play additional roles in spermatogenesis, other than in sperm physiology. Together with the high number of enriched TF motifs identified at differentially accessible ERVKs and LINE L1 elements, these data highlight a regulatory role for chromatin organization of TEs in SCs during the transition from development to adult stage (Sundaram et al., 2014 [↗](#); Sundaram and Wysocka, 2020 [↗](#)).

Limitations

One limitation of our study is the partial purity of SCs populations obtained by FACS, due to the fact that it does not fully remove other testicular cells from the samples. This therefore does not exclude the possible influence of contaminating cells on the data and their interpretation. Such influence may explain differences between our datasets and datasets in the literature. Nevertheless, by comparing chromatin landscape in developing and adult SCs, the study reveals an age-dependent dynamic reorganization of chromatin accessibility in these cells. When integrated with our transcriptomic datasets and published histone PTMs profiles, the data provide novel insight into transcriptome-chromatin dynamics of mouse SCs from early postnatal life to adulthood. This represents an important resource for future studies on mouse germ cells.

Mouse husbandry

Male C57Bl/6J mice were purchased from Janvier Laboratories (France) and bred in-house to C57Bl/6J primiparous females to generate males for the experiments. All animals were kept on a reversed 12-h light/12-h dark cycle in a temperature- and humidity-controlled facility with food (M/R Haltung Extrudat, Provimi Kliba SA, Switzerland) and water provided *ad libitum*. Cages were changed once weekly. Animals from 2 independent cohorts generated separately were used for the experiments.

Germ cells isolation

Germ cells were isolated at postnatal day (PND) 8 or 15 for RNA-seq and ATAC-seq, and at postnatal week 20 (adult) for ATAC-seq. Testicular single-cell suspensions were prepared as previously described with slight modifications (Kubota et al., 2004a, 2004b). For PND8 and PND15 cells, testes from 2 animals were pooled for each sample while for adults, testes from individual males were used. Pup testes were collected in sterile HBSS on ice. Tunica albuginea was gently removed from each testis, making sure to keep seminiferous tubules as intact as possible. Tubules were enzymatically digested in 0.25% trypsin-EDTA (ThermoFisher Scientific) and 7mg/ml DNase I (Sigma-Aldrich) solution for 5 min at 37°C. The suspension was vigorously pipetted up and down 10 times and incubated again for 3 min at 37°C. The digestion was stopped by adding 10% fetal bovine serum (ThermoFisher Scientific) and cells were passed through a 20µm-pore-size cell strainer (Miltenyi Biotec) and pelleted by centrifugation at 600g for 7 min at 4°C. Cells were resuspended in PBS-S (PBS with 1% PBS, 10 mM HEPES, 1 mM pyruvate, 1mg/ml glucose, 50 units/ml penicillin and 50 µg/ml streptomycin) and used for sorting. Adult testes were collected and the tunica was removed. Seminiferous tubules were digested in 1 mg/mL collagenase type IV (Sigma Aldrich) and then in 0.25 % Trypsin-EDTA (Gibco), both times for 8-12 minutes and in the presence of DNase I solution (Sigma Aldrich). FBS (Cytiva HyClone) was added to a concentration of 10 % and the cell suspension was filtered through a 40µm-pore-size cell strainer (Corning) and washed with DPBS-S (1 % FBS, 10 mM HEPES (Gibco), 1mM sodium pyruvate (Gibco), 1mg/mL Glucose (Gibco) and 1X Penicillin-Streptomycin (Gibco) in DPBS (Gibco). 5 mL of the single cell suspension was then overlaid on 2 mL 30 % Percoll (Sigma) and centrifuged with disabled break at 600g for 8 minutes at 4 °C. The supernatant was removed and cell suspension was washed twice in DPBS-S and used for sorting.

SCs enrichment by FACS

For pup testis, dissociated cells were stained with BV421-conjugated anti-β2M, biotin-conjugated anti-THY1 (53-2.1) and PE-conjugated anti-αv-integrin (RMV-7) antibodies. THY1 was detected by staining with Alexa Fluor 488-Sav. For adult testes, cells were stained with anti-α6-integrin (CD49f; GoH3), BV421-conjugated anti-β2 microglobulin (β2M; S19.8) and R-phycoerythrin (PE)-conjugated anti-THY1 (CD90.2; 30H-12) antibodies. α6-Integrin was detected by Alexa Fluor 488-Sav after staining with biotin-conjugated rat anti-mouse IgG1/2a (G28-5) antibody. Prior to FACS, 1 µg/ml propidium iodide (Sigma) was added to cell suspensions to discriminate dead cells. All antibody incubations were performed in PBS-S for at least 30 min at 4°C followed by washing in PBS-S. Antibodies were obtained from BD Biosciences (San Jose, United States) unless otherwise stated. Cell sorting was performed at 4°C on a FACS Aria III 5L using an 85µm nozzle at the Cytometry Facility of University of Zurich. For RNA-seq at PND8 and PND15, cells were collected in 1.5 ml Eppendorf tubes in 500 µL PBS-S, immediately pelleted by centrifugation and snap frozen in liquid N₂. Cell pellets were stored at -80°C until RNA extraction. For RNA-seq of adults, 1000 spermatogonial cells (MHC I negative, alpha-6-integrin and Thy1 positive) per male were sorted into PBS. For Omni-ATAC at PND15, 25'000 cells were collected in a separate tube, pelleted by

centrifugation and immediately processed using a library preparation protocol (Corces et al., 2017). For Omni-ATAC in adults, 5000 cells from each animal were collected in a separate tube and processed using the same protocol.

Immunocytochemistry

The protocol used for assessing SCs enrichment after sorting was kindly provided by Jon Oatley at Washington State University, Pullman, USA (Yang et al., 2013). Briefly, 30,000-50,000 cells were adhered to poly-L-Lysine coated coverslips (Corning Life Sciences) in 24-well plates for 1 h. Cells were fixed in freshly prepared 4% PFA for 10 min at room temperature then washed in PBS with 0.1% Triton X-100 (PBS-T). Non-specific antibody binding was blocked by incubation with 10% normal goat serum for 1 h at room temperature. Cells were incubated overnight at 4°C with mouse anti-PLZF (0.2 µg/ml, Active Motif) primary antibody. Alexa488 goat anti-mouse IgG (1 µg/mL, ThermoFisher Scientific) was used for secondary labelling at 4°C for 1 h. Coverslips were washed 3 times, mounted onto glass slides with VectaShield mounting medium containing DAPI (Vector Laboratories) and examined by fluorescence microscopy. SCs enrichment was determined by counting PLZF⁺ cells in 10 random fields of view from each coverslip and dividing by the total number of cells present in the same fields of view (DAPI-stained nuclei). The number of PLZF⁺ and PLZF⁻ cells from the 10 different fields of view was averaged.

RNA extraction and RNA-seq library preparation

For RNA-seq at PND8 and PND15, total RNA was extracted from sorted cells using AllPrep RNA/DNA Micro kit (Qiagen). RNA quality was assessed using a Bioanalyzer 2100 (Agilent Technologies). Samples were quantified using Qubit RNA HS Assay (ThermoFisher Scientific). RNA sequencing libraries were prepared using SMARTer Stranded Total RNA-Seq Kit v3 (Takara Bio USA, Inc) following the recommended protocol with minor adjustments. For PND8 and PND15 SCs libraries, RNA was fragmented for 4 minutes at 94 °C. After reverse transcription, samples were barcoded using SMARTer Unique Dual Index Kit (Takara Bio USA, Inc). Five PCR cycles were run and PCR products were purified using AMPure XP reagent (Beckman Coulter Life Sciences; bead:sample ratio 0.8X). Ribosomal cDNA was depleted following the protocol and final library amplification was performed with 12 PCR cycles. Libraries were purified twice using AMPure XP reagent (bead:sample ratio 1X) and eluted in Tris buffer. Adult SCs libraries were prepared using the option to start directly from cells (1000 cells as input). Cells were incubated for 6 minutes at 85 °C and processed as indicated for PND8 and PND15 SCs. Samples were pooled at equal molarity, as determined in a 100-800 bp window on the Bioanalyzer.

Omni-ATAC library preparation and sequencing

Chromatin accessibility was profiled from PND15 and adult SCs. Libraries were prepared according to Omni-ATAC protocol, starting from 25,000 PND15 and 5000 adult sorted SCs (Corces et al., 2017). Briefly, sorted cells were lysed in cold lysis buffer (10 mM Tris-HCl pH 7.4, 10 mM NaCl, 3 mM MgCl₂, 0.1% NP40, 0.1% Tween-20, and 0.01% digitonin) and nuclei were pelleted and transposed using Nextera Tn5 (Illumina) for 30 min at 37°C in a thermomixer with shaking at 1000 rpm. Transposed fragments were purified using MinElute Reaction Cleanup Kit (Qiagen). Following purification, libraries were generated by PCR amplification using NEBNext High-Fidelity 2X PCR Master Mix (New England Biolabs) and purified using Agencourt AMPure XP magnetic beads (Beckman Coulter) to remove primer dimers (78bp) and fragments of 1000-10,000 bp. Library quality was assessed on an Agilent High Sensitivity DNA chip using the Bioanalyzer 2100 (Agilent Technologies). 6 samples were sequenced from PND15 and 5 from adult SCs.

RNA-seq analysis

Quality control and alignment: 100bp single end sequencing was performed at the Functional Genomics Center Zurich (FGCZ) using a Novaseq SP flowcell on the Novaseq 6000 platform. Quality assessment of FASTQ files was done using FastQC (Andrews et al., 2012) (version 0.11.8).

TrimGalore (Krueger, 2015 [↗](#)) (version 0.6.2) was used to trim adapters and low-quality ends from reads with Phred score less than 30 (`-q 30`) and to discard trimmed reads shorter than 30bp (`--length 30`). Trimmed reads were pseudo-aligned using Salmon (Patro et al., 2017) (version 0.9.1) with automatic detection of the library type (`-l A`), correcting for sequence-specific bias (`--seqBias`) and correcting for fragment GC bias correction (`--gcBias`) on a transcript index prepared for the Mouse genome (GRCm38) from GENCODE (version M18) (Harrow et al., 2012 [↗](#)), with additional piRNA precursors and TEs (concatenated by family) from Repeat Masker as in (Gapp et al., 2018 [↗](#)).

Downstream analysis

Data analyses and plotting were conducted with R (R Core Team, 2020) (version 3.6.2) using packages from The Comprehensive R Archive Network (CRAN) (<https://cran.r-project.org> [↗](#)) and Bioconductor (Huber et al., 2015 [↗](#)). Pre-filtering of genes was done using the `filterByExpr` function from `edgeR` (Robinson et al., 2009 [↗](#)) (version 3.28.1) with a design matrix requiring at least 15 counts (`min.counts=15`). Normalization factors were obtained using TMM normalization (Robinson and Oshlack, 2010 [↗](#)) from `edgeR` package and differential gene expression analyses were done using `limma-voom` (Law et al., 2014 [↗](#)) pipeline from `limma` (Ritchie et al., 2015 [↗](#)) (version 3.42.2). GO enrichment analyses were performed using `g:Profiler` (<https://biit.cs.ut.ee/gprofiler/gost> [↗](#)) querying against *Mus musculus* database.

ATAC-seq analysis

Quality control, alignment, and peak calling: Paired-end (PE) sequencing was performed on PND15 and adult SCs on Illumina HiSeq2500 platform at FGCZ. FASTQ files were assessed for quality using FastQC (Andrews et al., 2012 [↗](#)) (version 0.11.8). QC was performed using TrimGalore (Krueger, 2015 [↗](#)) (version 0.6.2) in PE mode (`--paired`), trimming adapters, low-quality ends (`-q 30`) and discarding reads shorter than 30bp after trimming (`--length 30`). Alignment on GRCm38 genome was performed using Bowtie2 (Langmead and Salzberg, 2012 [↗](#)) (version 2.3.5) with the following parameters: allowing fragments up to 2kb to align (`-X 2000`), entire read alignment (`--end-to-end`), suppressing unpaired alignments for paired reads (`--no-mixed`), suppressing discordant alignments for paired reads (`--no-discordant`) and minimum acceptable alignment score with respect to read length (`--score-min L,-0.4,-0.4`). Using alignmentSieve (version 3.3.1) from deepTools (Ramirez et al., 2016 [↗](#)) (version 3.4.3), aligned data (BAM files) were adjusted for read start sites to represent the center of the transposon cutting event (`--ATACshift`), and filtered for reads with a high mapping quality (`--minMappingQuality 30`). Reads mapping to the mitochondrial chromosome and ENCODE blacklisted regions were filtered out. To call nucleosome-free regions, all aligned files were merged within groups (PND15 and adult), sorted and indexed using SAMtools (Li et al., 2009) (version 0.1.19) and nucleosome-free fragments (NFFs) were obtained by selecting alignments with a template length between 40 and 140bp in length. Peak calling on NFFs was performed using MACS2 (Zhang et al., 2008 [↗](#)) (version 2.2.7.1) with mouse genome size (`-g 2744254612`) and PE BAM file format (`-f BAMPE`).

Differential accessibility analysis

These analyses were conducted in R (version 3.6.2) using packages from CRAN (<https://cran.r-project.org> [↗](#)) and Bioconductor (Huber et al., 2015 [↗](#)). Peaks were annotated based on overlap with GENCODE (version M18) (Harrow et al., 2012 [↗](#)) transcript and/or distance to the nearest TSS (https://github.com/mansuylab/SC_postnatal_adult/bin/annoPeaks.R [↗](#)). The number of extended reads overlapping in peak regions was calculated using `csaw` package (Lun and Smyth, 2015 [↗](#)) (version 1.20.0). Peak regions that did not have at least 15 reads in at least 40% of the samples were filtered out. Normalization factors were obtained on filtered peak regions using TMM normalization method (Robinson and Oshlack, 2010 [↗](#)) and differential analysis on peaks (PND15

versus adult) was performed using Genewise Negative Binomial Generalized Linear Models with Quasi-likelihood (glmQLFit) Tests from edgeR package (Robinson et al., 2009) (version 3.28.1). Peak regions with an $\text{absLog}_2\text{FC} \geq 1$ and adjusted- $P \leq 0.05$ were categorized as DARs.

Downstream analysis

Heatmaps of normalized ATAC-seq signal were created using deepTools with default parameters. Genomic annotation of ATAC-seq peak and DARs and identification of closest gene DARs were performed using ChIPpeakAnno (Zhu et al., 2010). GO enrichment analysis of genes associated to DARs was performed using g:Profiler (Raudvere et al., 2019) querying against the *Mus musculus* database. For the epigenomic annotation of DARs, publicly available signal files and peak files for all histone marks were used (Cheng et al., 2020). Heatmaps of ChIP-seq signal for histone PTMs around ATAC-seq peaks and DARs were generated with deepTools. Overlap between ChIP-seq peaks and DARs was generated using Intervene (Khan et al., 2017). TF motif analysis was performed using MEME-ChIP (Ma et al., 2014) and motif identification was done querying identified motifs against JASPAR database (Castro-Mondragon et al., 2021). Quantification and identification of differences in chromatin accessibility between promoter regions of DEGs was performed with deepStats (Richard 2019). To quantify differences in chromatin accessibility between DEGs, bamscale cov (Pongor et al., 2020) was employed using ATAC-seq BAM files as input and genomic coordinates of up-regulated and down-regulated genes. Kruskal-Wallis test was used to test for significant differences in chromatin accessibility between each category of DEGs at postnatal and adult stage.

Differential accessibility analysis at TEs

TE gene transfer format (GTF) file was obtained from http://labshare.cshl.edu/shares/mhammellab/www-data/TEtranscripts/TE_GTF/mm10_rmsk_TE.gtf.gz on 03.02.2020. This file provides hierarchical information about TEs: Class (level 1, eg. LTR), family (level 2, eg. LTR ->L1), subtype (level 3, eg. LTR-> L1->L1_Rod), and locus (level 4, eg. LTR->L1 -> L1_Rod -> L1_Rod_dup1). TE loci were annotated based on overlap with GENCODE (version M18) as described above for ATAC-seq peaks. Filtered BAM files (without reads mapping to blacklisted or mitochondrial regions) were used to analyze TEs. Mapped reads were assigned to TEs using featureCounts from R package Rsubread (Liao et al., 2019) (version 2.0.1) and were summarized to Subtypes (level 3), allowing for multi-overlap with fractional counts, while ignoring duplicates. The number of extended reads overlapping at TE loci were obtained using csaw package (Lun and Smyth, 2015) (version 1.20.0). Subtypes without at least 15 reads, and loci without at least 5 reads in at least 40% of samples were filtered out. Normalization and differential accessibility analysis were performed as described above. Subtypes which had an absolute $\text{Log}_2\text{FC} \geq 0.5$ and adjusted- $P \leq 0.05$ were categorized as differentially accessible subtypes and loci with an $\text{absLog}_2\text{FC} \geq 1$ and adjusted- $P \leq 0.05$ were categorized as differentially accessible loci. For further downstream data analysis, only differentially accessible loci or differentially accessible subtypes were considered. TF motif enrichment analysis was performed using the marge package (Amezquita, 2018) (version 0.0.4.9999), which is a wrapper around the Homer tool (Heinz et al., 2010) (version 4.11.1).

Authors contribution

ILC and IMM designed and conceived the study. ILC performed all RNA-seq, ICC and ATAC-seq experiments with support of LCS. DKT and RGA-M analyzed the RNA-seq, ATAC-seq, ChIP-seq with significant support from PLG. OUF and MC performed chromatin accessibility analysis of DEGs. ILC, DKT and RGA-M prepared figures. ILC and RGA-M interpreted the data with significant input from DKT, PLG and IMM. ILC, DKT, RGA-M and IMM wrote the manuscript, with significant input from PLG. All authors read and accepted the final version of the manuscript.

Acknowledgements

We thank Martin Roszkowski and Francesca Manuella for taking care of animals breeding, Yvonne Zipfel for animal care, Silvia Schelbert and Alberto Corcoba for taking care of animal licenses and lab organization. We thank Catherine Aquino and Emilio Yánguez from Functional Genomics Center Zurich for support and advice with libraries preparation and sequencing. We are very grateful to Jon Oatley, Melissa Oatley, Tessa Lord and Nathan Law for conceptual advice, hands-on training, and for providing detailed protocols for testis dissection and preparation, and immunocytochemistry of SCs. We thank Zuguang Gu for support with heatmaps. We thank Service and Support for Science IT (www.s3it.uzh.ch) for computational infrastructure.

Competing interest

The authors declare that they have no competing interests.

Funding

The Mansuy lab is funded by the University Zürich, the ETH Zürich, the Swiss National Science Foundation grant number 31003A_175742/1, the National Centre of Competence in Research (NCCR) RNA&Disease funded by the Swiss National Science Foundation (grant number 182880/Phase 2 and 205601/Phase 3), ETH grants (ETH-10 15-2 and ETH-17 13-2), European Union Horizon 2020 Research Innovation Program Grant number 848158, European Union projects FAMILY and HappyMums funded by the Swiss State Secretariat for Education, Research and Innovation (SERI), FreeNovation grant from Novartis Forschungsstiftung, and the Escher Family Fund. RGA-M received an ETH Postdoctoral Fellow grant number 20-1 FEL-28. DKT received a Swiss Government Excellence Scholarship.

Data and material availability

Sequencing data is available via the EBI BioStudies database within the ArrayExpress collection (RNA-seq: E-MTAB-12721; ATAC-seq: E-MTAB-12722). The code employed for data analysis is available from https://github.com/mansuylab/SC_postnatal_adult/. Additional information is available upon request.

Supplementary Figure 1. Expression of SCs markers and their dynamics between early postnatal and adult stage.

(A) Heatmap of the expression profile of an extended list of selected markers of spermatogonial and different testicular somatic cells extracted from total RNA-seq data on PND8, PND15 and adult samples (n=6 for each group). Each row in the heatmap represents a biological replicate from two experimental batches. Gene names in bold correspond to cellular markers presented in **Figure 1C**. Gene expression is represented as Log₂CPM (counts per million).

(B) *Left*, Heatmap of the expression profile of genes involved in germ-cell maintenance, pluripotency and signalling as reported by Hammoud, 2015. Each row in the heatmap represents a biological replicate from two experimental batches. Unsupervised hierarchical clustering was applied to each of the rows of the heatmaps and a dendrogram indicating similarity of expression

profiles among genes in each biological category is shown with each heatmap. *Right*, line-plots of the average expression of each gene displayed in the heatmaps showing the dynamics and breadth of gene expression across SCs postnatal development.

(C) Genomic snapshots from IVG of exemplary DEGs showing aggregated RNA-seq signal from PND8, PND15 and adult stages.

(D) *Left*, bar-plot of GO KEGG pathways categories enriched in DEGs between PND15 and adult SCs (adjusted- $P \leq 0.05$). Dotted line indicates a threshold value for significance of 0.05. *Right*, Heatmap of DEGs between PND8 and PND15 belonging to the GO category “ECM-receptor interaction”. Each row in the heatmap represents a biological replicate from two experimental batches. Shown are Log₂FC with respect to the average of PND8.

Supplementary Figure 2. Specific transcriptional programs between postnatal and adult SCs.

(A) Four-way Venn diagram of DEGs detected between PND8-PND15 and PND15-adult comparisons.

(B) Heatmap of all DEGs specific to PND8 stage. Each row in the heatmap represents a biological replicate from two experimental batches. Shown are the Log₂ FC with respect to the average of PND8.

(C) Heatmap of all DEGs with significant changes across the 3 developmental time points. Each row in the heatmap represents a biological replicate from two experimental batches. Shown are the Log₂ FC with respect to the average of PND8.

Supplementary Figure 3. Chromatin accessibility landscape of SCs from PND15 to adult stage.

(A) Heatmaps showing normalized ATAC-seq signal for all identified ATAC-seq peaks from PND15 and adult stages. Each row in the heatmap represents a 2kb genomic region extended 1kb down- and upstream from the center of each identified peak. Each row is ordered in a decreasing level of average accessibility. On top of each heatmap is shown a plot of the signal profile over all ATAC-seq peaks and their extended genomic region.

(B) Bar plot of the genomic distribution of all identified ATAC-seq peaks from PND15 and adult stages.

(C) IGV tracks for ATAC-seq signal for PND15 and adult SCs showing ATAC-seq peaks located at promoters and intragenic regions of genes with important functions in SCs. Highlighted genomic segments correspond to ATAC-seq peaks.

(D) Heatmaps showing normalized ChIP-seq signal for different histone marks in adult SCs (public data derived from [Cheng et al., 2020](#) [🔗](#)) at DARs from PND15 and adult stages. Each row in the heatmap represents a 2kb genomic region extended 1kb down- and upstream from the centre of each identified peak. Shown data corresponds to non-regenerative SCs as stated in [Cheng et al., 2020](#) [🔗](#).

References

- Amezquita RA. (2018) **marge: An API for Analysis of Motifs Using HOMER in R** *bioRxiv* <https://doi.org/10.1101/249268>
- An Z, Liu P, Zheng J, Si C, Li T, Chen Y, Ma T, Zhang MQ, Zhou Q, Ding S (2019) **Sox2 and Klf4 as the Functional Core in Pluripotency Induction without Exogenous Oct4** *Cell Rep* **29**:1986–2000
- Andrews S, Krueger F, Segonds-Pichon A, Biggins L, Krueger C, Wingett S. (2012) **FastQC. A quality control tool for high throughput sequence data**
- Argelaguet R *et al.* (2019) **Multi-omics profiling of mouse gastrulation at single-cell resolution** *Nature* **576**:487–491
- Arzate-Mejia RG, Mansuy IM (2023) **Remembering through the genome: the role of chromatin states in brain functions and diseases** *Translational Psychiatry* **13**:1–11
- Atlasi YS, Stunnenberg H (2017) **The interplay of epigenetic marks during stem cell differentiation and development** *Nat Rev Genet* **18**:643–658
- Barber MF *et al.* (2012) **SIRT7 links H3K18 deacetylation to maintenance of oncogenic transformation** *Nature* **487**:114–118
- Barisic D, Stadler MB, Iurlaro M, Schübeler D (2019) **Mammalian ISWI and SWI/SNF selectively mediate binding of distinct transcription factors** *Nature* **569**:136–140
- Bejjani F, Evanno E, Zibara K, Piechaczyk M, Jariel-Encontre I (2019) **The AP-1 transcriptional complex: Local switch or remote command?** *Biochimica et Biophysica Acta (BBA) - Reviews on Cancer* **1872**:11–23
- Bergmann JH, Li J, Eckersley-Maslin MA, Rigo F, Freier SM, Spector DL (2015) **Regulation of the ESC transcriptome by nuclear long noncoding RNAs** *Genome Res* **25**:1336–1346
- Bernardino RL, Alves MG, Oliveira PF (2018) **Evaluation of the purity of sertoli cell primary cultures** *Methods in Molecular Biology* **1748**:9–15
- Bialkowska AB, Yang VW, Mallipattu SK (2017) **Krüppel-like factors in mammalian stem cells and development** *Development* **144**
- Bleckwehl T *et al.* (2021) **Enhancer-associated H3K4 methylation safeguards in vitro germline competence** *Nature Communications* **2021**:1–19
- Cao C, Ma Q, Mo S, Shu G, Liu Q, Ye J, Gui Y (2021) **Single-Cell RNA Sequencing Defines the Regulation of Spermatogenesis by Sertoli-Cell Androgen Signaling** *Front Cell Dev Biol* **9**
- Castro-Mondragon JA *et al.* (2022) **JASPAR 2022: the 9th release of the open-access database of transcription factor binding profiles** *Nucleic Acids Res* **50**:D165–D173
- Chakraborty P, Buaas FW, Sharma M, Snyder E, de Rooij DG, Braun RE. (2014) **LIN28A marks the spermatogonial progenitor population and regulates its cyclic expansion** *Stem Cells* **32**

Cheng K, Chen IC, Cheng CHE, Mutoji K, Hale BJ, Hermann BP, Geyer CB, Oatley JM, McCarrey JR. (2020) **Unique Epigenetic Programming Distinguishes Regenerative Spermatogonial Stem Cells in the Developing Mouse Testis** *iScience*

Chereji R V., Eriksson PR, Ocampo J, Prajapati HK, Clark DJ (2019) **Accessibility of promoter DNA is not the primary determinant of chromatin-mediated gene regulation** *Genome Res* **29**:1985–1995

Choksi SP, Lauter G, Swoboda P, Roy S (2014) **Switching on cilia: transcriptional networks regulating ciliogenesis** *Development* **141**:1427–1441

Chu JS, Baillie DL, Chen N (2010) **Convergent evolution of RFX transcription factors and ciliary genes predated the origin of metazoans** *BMC Evol Biol* **10**

Corces MR *et al.* (2017) **An improved ATAC-seq protocol reduces background and enables interrogation of frozen tissues** *Nat Methods* **14**:959–962

Costoya JA, Hobbs RM, Barna M, Cattoretti G, Manova K, Sukhwani M, Orwig KE, Wolgemuth DJ, Pandolfi PP (2004) **Essential role of Plzf in maintenance of spermatogonial stem cells** *Nat Genet* **36**:653–659

Dalton S, Treisman R (1992) **Characterization of SAP-1, a protein recruited by serum response factor to the c-fos serum response element** *Cell* **68**:597–612

Dann CT, Alvarado AL, Molyneux LA, Denard BS, Garbers DL, Porteus MH (2008) **Spermatogonial Stem Cell Self-Renewal Requires OCT4, a Factor Downregulated During Retinoic Acid-Induced Differentiation** *Stem Cells* **26**:2928–2937

Davis MP *et al.* **Shkumatava A**

Enright AJ D (2017) **Transposon-driven transcription is a conserved feature of vertebrate spermatogenesis and transcript evolution** *EMBO Rep* **18**:1231–1247

De Rooij DG. (2017) **The nature and dynamics of spermatogonial stem cells** *Development (Cambridge)* <https://doi.org/10.1242/dev.146571>

Deniz Ö, Frost JM, Branco MR (2019) **Regulation of transposable elements by DNA modifications** *Nat Rev Genet* <https://doi.org/10.1038/s41576-019-0106-6>

Edwards JR, Yarychkivska O, Boulard M, Bestor TH (2017) **DNA methylation and DNA methyltransferases** *Epigenetics Chromatin* **10**:1–10

Fort A *et al.* (2014) **Deep transcriptome profiling of mammalian stem cells supports a regulatory role for retrotransposons in pluripotency maintenance** *Nat Genet* **46**:558–566

Fukuda N, Touhara K (2005) **Developmental expression patterns of testicular olfactory receptor genes during mouse spermatogenesis** *Genes to Cells* **11**:71–81

Gapp K *et al.* (2018) **Alterations in sperm long RNA contribute to the epigenetic inheritance of the effects of postnatal trauma** *Molecular Psychiatry* **25**:2162–2174

Gasperini M, Tome JM, Shendure J (2020) **Towards a comprehensive catalogue of validated and target-linked human enhancers** *Nature Reviews Genetics* **2020**:292–310

Gewiss RL, Law NC, Hesel AR, Shelden EA, Griswold MD (2021) **Two distinct Sertoli cell states are regulated via germ cell crosstalk** *Biol Reprod* **105**

Goertz MJ, Wu Z, Gallardo TD, Hamra FK, Castrillon DH (2011) **Foxo1 is required in mouse spermatogonial stem cells for their maintenance and the initiation of spermatogenesis** *J Clin Invest* **121**:3456–3466

Green CD *et al.* (2018) **A Comprehensive Roadmap of Murine Spermatogenesis Defined by Single-Cell RNA-Seq** *Dev Cell* **46**:651–667

Grive KJ, Hu Y, Shu E, Grimson A, Elemento O, Grenier JK, Cohen PE (2019) **Dynamic transcriptome profiles within spermatogonial and spermatocyte populations during postnatal testis maturation revealed by single-cell sequencing** *PLoS Genet* **15**

Guo J, Grow EJ, Yi C, Goriely A, Hotaling JM, Cairns Correspondence BR (2017) **Chromatin and Single-Cell RNA-Seq Profiling Reveal Dynamic Signaling and Metabolic Transitions during Human Spermatogonial Stem Cell Development** *Cell Stem Cell* **21**:533–546

Haggerty C *et al.* (2021) **Dnmt1 has de novo activity targeted to transposable elements** *Nature Structural & Molecular Biology* **2021**:594–603

Hammoud SS, Low DHP, Yi C, Carrell DT, Guccione E, Cairns BR (2014) **Chromatin and Transcription Transitions of Mammalian Adult Germline Stem Cells and Spermatogenesis** *Cell Stem Cell* **15**:239–253

Hammoud SS, Low DHP, Yi C, Lee CL, Oatley JM, Payne CJ, Carrell DT, Guccione E, Cairns BR (2015) **Transcription and imprinting dynamics in developing postnatal male germline stem cells** *Genes Dev* **29**:2312–24

Harrow J *et al.* (2012) **GENCODE: The reference human genome annotation for the ENCODE project** *Genome Research* **22**:1760–1774

He Z, Feng L, Zhang X, Geng Y, Parodi DA, Suarez-Quian C, Dym M (2005) **Expression of Col1a1, Col1a2 and procollagen I in germ cells of immature and adult mouse testis** *Reproduction* **130**:333–341

He Z, Jiang J, Hofmann M-C, Dym M (2007) **Gfra1 Silencing in Mouse Spermatogonial Stem Cells Results in Their Differentiation Via the Inactivation of RET Tyrosine Kinase 1** *Biol Reprod* **77**:723–733

He Z, Jiang J, Kokkinaki M, Golestaneh N, Hofmann M-C, Dym M (2008) **Gdnf upregulates c-Fos transcription via the Ras/Erk1/2 pathway to promote mouse spermatogonial stem cell proliferation** *Stem Cells* **26**:266–278

Heintzman ND *et al.* (2009) **Histone modifications at human enhancers reflect global cell-type-specific gene expression** *Nature* **459** <https://doi.org/10.1038/nature07829>

Hesel AR, Yang QE, Oatley MJ, Lord T, Sablitzky F, Oatley JM (2017) **ID4 levels dictate the stem cell state in mouse spermatogonia** *Development* **144**:624–634

Henikoff S, Henikoff JG, Kaya-Okur HS, Ahmad K (2020) **Efficient chromatin accessibility mapping in situ by nucleosome-tethered tagmentation** *Elife* **9**:1–19

- Hermann BP *et al.* (2018) **The Mammalian Spermatogenesis Single-Cell Transcriptome, from Spermatogonial Stem Cells to Spermatids** *Cell Rep* **25**:1650–1667
- Hu Q *et al.* (2021) **GPX4 and vitamin E cooperatively protect hematopoietic stem and progenitor cells from lipid peroxidation and ferroptosis** *Cell Death & Disease* **12**:1–9
- Huber W *et al.* (2015) **Orchestrating high-throughput genomic analysis with Bioconductor** *Nature Methods* **12**:115–121
- Kaluscha S, Domcke S, Wirbelauer C, Stadler MB, Durdu S, Burger L, Schübeler D (2022) **Evidence that direct inhibition of transcription factor binding is the prevailing mode of gene and repeat repression by DNA methylation** *Nature Genetics* **54**:1895–1906
- Kanatsu-Shinohara M, Naoki H, Tanaka T, Tatehana M, Kikkawa T, Osumi N, Shinohara T (2022) **Regulation of male germline transmission patterns by the Trp53-Cdkn1a pathway** *Stem Cell Reports* **17**:1924–1941
- Kawase S, Kuwako K, Imai T, Renault-Mihara F, Yaguchi K, Itohara S, Okano H (2014) **Regulatory Factor X Transcription Factors Control Musashi1 Transcription in Mouse Neural Stem/Progenitor Cells** *Stem Cells Dev* **23**
- Khan A, Mathelier A (2017) **Intervene: a tool for intersection and visualization of multiple gene or genomic region sets** *BMC Bioinformatics* **18**
- Kiani K, Sanford EM, Goyal Y, Raj A (2022) **Changes in chromatin accessibility are not concordant with transcriptional changes for single-factor perturbations** *Mol Syst Biol* **18**
- Klemm SL, Shipony Z, Greenleaf WJ (2019) **Chromatin accessibility and the regulatory epigenome** *Nature Reviews Genetics* **20**:207–220
- Krueger F. (2015) **Trim Galore. A wrapper tool around Cutadapt and FastQC to consistently apply quality and adapter trimming to FastQ files**
- Kubota H, Avarbock MR, Brinster RL (2004) **Culture Conditions and Single Growth Factors Affect Fate Determination of Mouse Spermatogonial Stem Cells** *Biol Reprod* **71**:722–731
- Kubota H, Brinster RL (2018) **Spermatogonial stem cells** *Biol Reprod* <https://doi.org/10.1093/biolre/iroy077>
- Langmead B, Salzberg SL. (2012) **Fast gapped-read alignment with Bowtie 2** *Nature Methods* **9**:357–359
- Law CW, Chen Y, Shi W, Smyth GK (2014) **voom: precision weights unlock linear model analysis tools for RNA-seq read counts** *Genome Biology* **15**
- Law NC, Oatley MJ, Oatley JM (2019) **Developmental kinetics and transcriptome dynamics of stem cell specification in the spermatogenic lineage** *Nat Commun* **10**
- Liao Y, Smyth GK, Shi W (2019) **The R package Rsubread is easier, faster, cheaper and better for alignment and quantification of RNA sequencing reads** *Nucleic Acids Research* **47**:e47–e47
- Lu JY *et al.* (2020) **Genomic Repeats Categorize Genes with Distinct Functions for Orchestrated Regulation** *Cell Rep* **30**:3296–3311

Lun ATL, Smyth GK (2015) **csaw: a Bioconductor package for differential binding analysis of ChIP-seq data using sliding windows** *Nucleic Acids Research* **44**

Ma W, Noble W, Bailey T (2014) **Motif-based analysis of large nucleotide data sets using MEME-ChIP** *Nat Protoc* **9**:1428–1450

Marco A *et al.* (2020) **Mapping the epigenomic and transcriptomic interplay during memory formation and recall in the hippocampal engram ensemble** *Nature Neuroscience* **2020**:1606–1617

Matson CK, Murphy MW, Griswold MD, Yoshida S, Bardwell VJ, Zarkower D (2010) **The mammalian Doublesex homolog DMRT1 is a transcriptional gatekeeper that controls the mitosis versus meiosis decision in male germ cells** *Dev Cell* **19**

McCarrey JR (2023) **Epigenetic priming as a mechanism of predetermination of spermatogonial stem cell fate** *Andrology* **11**:918–926

Nichols J, Zevnik B, Anastassiadis K, Niwa H, Klewe-Nebenius D, Chambers I, Schöler H, Smith A (1998) **Formation of pluripotent stem cells in the mammalian embryo depends on the POU transcription factor Oct4** *Cell* **95**:379–391

Oatley JM, Griswold MD (2017) **The biology of mammalian spermatogonia** *The Biology of Mammalian Spermatogonia* <https://doi.org/10.1007/978-1-4939-7505-1>

Oldfield AJ, Yang P, Conway AE, Cinghu S, Freudenberg JM, Yellaboina S, Jothi R (2014) **Histone-Fold Domain Protein NF-Y Promotes Chromatin Accessibility for Cell Type-Specific Master Transcription Factors** *Mol Cell* **55**:708–722

Pongor LS *et al.* (2020) **BAMscale: quantification of next-generation sequencing peaks and generation of scaled coverage tracks** *Epigenetics & Chromatin* **13**

Prado F, Jimeno-González S, Reyes JC (2017) **Histone availability as a strategy to control gene expression** *RNA Biology* **14**:281–286

Quigley IK, Kintner C (2017) **Rfx2 Stabilizes Foxj1 Binding at Chromatin Loops to Enable Multiciliated Cell Gene Expression** *PLoS Genet* **13**

Rada-Iglesias A, Bajpai R, Swigut T, Brugmann SA, Flynn RA, Wysocka J (2011) **A unique chromatin signature uncovers early developmental enhancers in humans** *Nature* **470**

Ramirez F, Ryan DP, Grüning B, Bhardwaj V, Kilpert F, Richter AS, Heyne S, Dündar F, Manke T (2016) **deepTools2: a next generation web server for deep-sequencing data analysis** *Nucleic Acids Research* **44**:W160–W165

Raudvere U, Kolberg L, Kuzmin I, Arak T, Adler P, Peterson H, Vilo J (2019) **g:Profiler: a web server for functional enrichment analysis and conversions of gene lists** *Nucleic Acids Research* **47**:W191–W198

Reissig LF *et al.* (2019) **The Col4a2em1(IMPC)Wtsi mouse line: Lessons from the Deciphering the Mechanisms of Developmental Disorders program** *Biol Open* **8**

Richard G. (2019) **gtrichard/deepStats: deepStats 0.3.1 (Version 0.3.1)**. Zenodo <https://doi.org/10.5281/zenodo.3336593>

- Ritchie ME, Phipson B, Wu D, Hu Y, Law CW, Shi W, Smyth GK (2015) **limma powers differential expression analyses for RNA-sequencing and microarray studies** *Nucleic Acids Research* **43**:e47–e47
- Robinson MD, McCarthy DJ, Smyth GK (2009) **edgeR: a Bioconductor package for differential expression analysis of digital gene expression data** *Bioinformatics* **26**:139–140
- Robinson MD, Oshlack A (2010) **A scaling normalization method for differential expression analysis of RNA-seq data** *Genome Biology* **11**
- Sakashita A, Maezawa S, Alavattam K, Yukawa M, Barski A, Pavlicev M, Namekawa S (2020) **Endogenous retroviruses drive species-specific germline transcriptomes in mammals** *Nat Struct Mol Biol* **27**:967–977
- Sararols P, Stévant I, Neirijnck Y, Rebourcet D, Darbey A, Curley MK, Kühne F, Dermitzakis E, Smith LB, Nef S (2021) **Specific Transcriptomic Signatures and Dual Regulation of Steroidogenesis Between Fetal and Adult Mouse Leydig Cells** *Front Cell Dev Biol* **9**
- Schrans-Stassen BHGJ, van de Kant HJG, de Rooij DG, van Pelt AMM. (1999) **Differential expression of c-kit in mouse undifferentiated and differentiating type A spermatogonia** *Endocrinology* **140**:5894–5900
- Shaulian E, Karin M (2002) **AP-1 as a regulator of cell life and death** *Nat Cell Biol* **4**:E131–E136
- Shlyueva D, Stampfel G, Stark A (2014) **Transcriptional enhancers: from properties to genome-wide predictions** *Nature Reviews Genetics* **2014**:272–286
- Song W, Shi X, Xia Q, Yuan M, Liu J, Hao K, Qian Y, Zhao X, Zou K (2020) **PLZF suppresses differentiation of mouse spermatogonial progenitor cells via binding of differentiation associated genes** *J Cell Physiol* **235**:3033–3042
- Sun F, Xu Q, Zhao D, Chen CD (2015) **Id4 Marks Spermatogonial Stem Cells in the Mouse Testis** *Scientific Reports* **5**
- Sun Z, Zhu M, Lv P, Cheng L, Wang Q, Tian P, Yan Z, Wen B (2018) **The Long Noncoding RNA Lncenc1 Maintains Naive States of Mouse ESCs by Promoting the Glycolysis Pathway** *Stem Cell Reports* **11**:741–755
- Sundaram V, Cheng Y, Ma Z, Li D, Xing X, Edge P, Snyder MP, Wang T (2014) **Widespread contribution of transposable elements to the innovation of gene regulatory networks** *Genome Res* **24**:1963–1976
- Sundaram V, Wysocka J (2020) **Transposable elements as a potent source of diverse cis-regulatory sequences in mammalian genomes** *Philosophical Transactions of the Royal Society B: Biological Sciences* <https://doi.org/10.1098/rstb.2019.0347>
- Tang L, Wang M, Liu D, Gong M, Ying QL, Ye S (2017) **Sp5 induces the expression of Nanog to maintain mouse embryonic stem cell self-renewal** *PLoS One* **12**
- Thompson PJ, Macfarlan TS, Lorincz MC (2016) **Long Terminal Repeats: From Parasitic Elements to Building Blocks of the Transcriptional Regulatory Repertoire** *Mol Cell* <https://doi.org/10.1016/j.molcel.2016.03.029>

Ueda A, Akagi T, Yokota T (2017) **GA-Binding Protein Alpha Is Involved in the Survival of Mouse Embryonic Stem Cells** *Stem Cells* **35**:2229–2238

Vierbuchen T, Ling E, Cowley CJ, Couch CH, Wang X, Harmin DA, Roberts CWM, Greenberg ME (2017) **AP-1 Transcription Factors and the BAF Complex Mediate Signal-Dependent Enhancer Selection** *Mol Cell* **68**:1067–1082

Wang M *et al.* (2018) **Single-Cell RNA Sequencing Analysis Reveals Sequential Cell Fate Transition during Human Spermatogenesis** *Cell Stem Cell* **23**:599–614

Mei Wang, Yu L, Wang S, Yang F, Min Wang, Li L, Wu X (2020) **LIN28A binds to meiotic gene transcripts and modulates their translation in male germ cells** *J Cell Sci* **133**

Wu F, Liu Y, Wu Q, Li D, Zhang L, Wu X, Wang R, Zhang D, Gao S, Li W (2018) **Long non-coding RNAs potentially function synergistically in the cellular reprogramming of SCNT embryos** *BMC Genomics* **19**

Wu X, Oatley JM, Oatley MJ, Kaucher A V., Avarbock MR, Brinster RL (2010) **The POU domain transcription factor POU3F1 is an important intrinsic regulator of GDNF-induced survival and self-renewal of mouse spermatogonial stem cells** *Biol Reprod* **82**:1103–1111

Xiong L *et al.* (2022) **Oct4 differentially regulates chromatin opening and enhancer transcription in pluripotent stem cells** *Elife* **11** <https://doi.org/10.7554/ELIFE.71533>

Yamane M, Ohtsuka S, Matsuura K, Nakamura A, Niwa H (2018) **Overlapping functions of krüppel-like factor family members: Targeting multiple transcription factors to maintain the naïve pluripotency of mouse embryonic stem cells** *Development (Cambridge)* **145**

Zhang T, Oatley J, Bardwell VJ, Zarkower D (2016) **DMRT1 Is Required for Mouse Spermatogonial Stem Cell Maintenance and Replenishment** *PLoS Genet* **12**

Zhang Y *et al.* (2008) **Model-based Analysis of ChIP-Seq (MACS)** *Genome Biology* **9**

Zhu L, Gazin C, Lawson N, Pagès H, Lin S, Lapointe D, Green M (2010) **ChIPpeakAnno: a Bioconductor package to annotate ChIP-seq and ChIP-chip data** *BMC Bioinformatics* **11**

Article and author information

Irina Lazar-Contes

Laboratory of Neuroepigenetics, Brain Research Institute, Medical Faculty of the University of Zurich and Institute for Neuroscience, Department of Health Science and Technology of the ETH Zurich, Zurich, Switzerland, Center for Neuroscience Zurich, ETH and University Zurich
ORCID iD: [0000-0002-8339-1267](https://orcid.org/0000-0002-8339-1267)

Deepak K. Tanwar

Laboratory of Neuroepigenetics, Brain Research Institute, Medical Faculty of the University of Zurich and Institute for Neuroscience, Department of Health Science and Technology of the ETH Zurich, Zurich, Switzerland, Center for Neuroscience Zurich, ETH and University Zurich
ORCID iD: [0000-0001-8036-1989](https://orcid.org/0000-0001-8036-1989)

Rodrigo G. Arzate-Mejia

Laboratory of Neuroepigenetics, Brain Research Institute, Medical Faculty of the University of Zurich and Institute for Neuroscience, Department of Health Science and Technology of the ETH Zurich, Zurich, Switzerland, Center for Neuroscience Zurich, ETH and University Zurich

Leonard C. Steg

Laboratory of Neuroepigenetics, Brain Research Institute, Medical Faculty of the University of Zurich and Institute for Neuroscience, Department of Health Science and Technology of the ETH Zurich, Zurich, Switzerland, Center for Neuroscience Zurich, ETH and University Zurich

Olivier Ulrich Feudjio

ADLIN Science, Pépinière «Genopole Entreprises», Evry, France

Marion Crespo

ADLIN Science, Pépinière «Genopole Entreprises», Evry, France

Pierre-Luc Germain

Laboratory of Neuroepigenetics, Brain Research Institute, Medical Faculty of the University of Zurich and Institute for Neuroscience, Department of Health Science and Technology of the ETH Zurich, Zurich, Switzerland, Center for Neuroscience Zurich, ETH and University Zurich
ORCID iD: [0000-0003-3418-4218](https://orcid.org/0000-0003-3418-4218)

Isabelle M. Mansuy

Laboratory of Neuroepigenetics, Brain Research Institute, Medical Faculty of the University of Zurich and Institute for Neuroscience, Department of Health Science and Technology of the ETH Zurich, Zurich, Switzerland, Center for Neuroscience Zurich, ETH and University Zurich
For correspondence: mansuy@hifo.uzh.ch
ORCID iD: [0000-0001-7785-5371](https://orcid.org/0000-0001-7785-5371)

Copyright

© 2023, Lazar-Contes et al.

This article is distributed under the terms of the [Creative Commons Attribution License](https://creativecommons.org/licenses/by/4.0/), which permits unrestricted use and redistribution provided that the original author and source are credited.

Editors

Reviewing Editor

Wei Yan

University of California, Los Angeles, United States of America

Senior Editor

Wei Yan

University of California, Los Angeles, United States of America

Reviewer #1 (Public Review):

Summary:

The authors appear to be attempting to describe dynamic changes in the chromatin landscape in spermatogonial cells during postnatal development ranging from prepubertal

stages at postnatal days 8 or 15 to adult stages. The authors attempt to relate differences they observe in chromatin accessibility at these different stages to changes in gene expression to better understand the molecular mechanisms regulating this differential gene expression.

Strengths:

The primary strength of the manuscript is that it provides additional datasets describing gene expression and chromatin accessibility patterns in spermatogonial cells at different postnatal ages.

Weaknesses:

There appears to be a lack of basic knowledge of the process of spermatogenesis. For instance, the statement that "During the first week of postnatal life, a population of SCs continues to proliferate to give rise to undifferentiated A single (As), A paired (Apr) and A aligned (Aal) cells. The remaining SCs differentiate to form chains of daughter cells that become primary and secondary permatocytes around postnatal day (PND) 10 to 12." is inaccurate. The Aal cells are the spermatogonial chains, the two are not distinct from one another. In addition, the authors fail to mention spermatogonial stem cells which form the basis for steady-state spermatogenesis. The authors also do not acknowledge the well-known fact that, in the mouse, the first wave of spermatogenesis is distinct from subsequent waves. Finally, the authors do not mention the presence of both undifferentiated spermatogonia (aka - type A) and differentiating spermatogonia (aka - type B). The premise for the study they present appears to be the implication that little is known about the dynamics of chromatin during the development of spermatogonia. However, there are published studies on this topic that have already provided much of the information that is presented in the current manuscript.

It is not clear which spermatogonial subtype the authors intended to profile with their analyses. On the one hand, they used PLZF to FACS sort cells. This typically enriches for undifferentiated spermatogonia. On the other hand, they report detection in the sorted population of markers such as c-KIT which is a well-known marker of differentiating spermatogonia, and that is in the same population in which ID4, a well-known marker of spermatogonial stem cells, was detected. The authors cite multiple previously published studies of gene expression during spermatogenesis, including studies of gene expression in spermatogonia. It is not at all clear what the authors' data adds to the previously available data on this subject.

The authors analyzed cells recovered at PND 8 and 15 and compared those to cells recovered from the adult testis. The PND 8 and 15 cells would be from the initial wave of spermatogenesis whereas those from the adult testis would represent steady-state spermatogenesis. However, as noted above, there appears to be a lack of awareness of the well-established differences between spermatogenesis occurring at each of these stages.

In general, the authors present observational data of the sort that is generated by RNA-seq and ATAC-seq analyses, and they speculate on the potential significance of several of these observations. However, they provide no definitive data to support any of their speculations. This further illustrates the fact that this study contributes little if any new information beyond that already available from the numerous previously published RNA-seq and ATAC-seq studies of spermatogenesis. In short, the study described in this manuscript does not advance the field.

The phenomenon of epigenetic priming is discussed, but then it seems that there is some expression of surprise that the data demonstrate what this reviewer would argue are examples of that phenomenon. The authors discuss the "modest correspondence between transcription and chromatin accessibility in SCs." Chromatin accessibility is an example of an epigenetic parameter associated with the primed state. The primed state is not fully equivalent to the actively expressing state. It appears that certain histone modifications along

with transcription factors are critical to the transition between the primed and actively expressing states (in either direction). The cell types that were investigated in this study are closely related spermatogenic, and predominantly spermatogonial cell types. It is very likely that the differentially expressed loci will be primed in both the early (PND 8 or 15) and adult stages, even though those genes are differentially expressed at those stages. Thus, it is not surprising that there is not a strict concordance between +/- chromatin accessibility and +/- active or elevated expression.

Reviewer #2 (Public Review):

The objective of this study from Lazar-Contes et al. is to examine chromatin accessibility changes in "spermatogonial cells" (SCs) across testis development. Exactly what SCs are, however, remains a mystery. The authors mention in the abstract that SCs are undifferentiated male germ cells and have self-renewal and differentiation activity, which would be true for Spermatogonial STEM Cells (SSCs), a very small subset of total spermatogonia, but then the methods they use to retrieve such cells using antibodies that enrich for undifferentiated spermatogonia encompass both undifferentiated and differentiating spermatogonia. Data in Fig. 1B prove that most (85-95%) are PLZF+, but PLZF is known to be expressed both by undifferentiated and differentiating (KIT+) spermatogonia (Niederberger et al., 2015; PMID: 25737569). Thus, the bulk RNA-seq and ATAC-seq data arising from these cells constitute the aggregate results comprising the phenotype of a highly heterogeneous mixture of spermatogonia (plus contaminating somatic cells), NOT SSCs. Indeed, Fig. 1C demonstrates this by showing the detection of Kit mRNA (a well-known marker of differentiating spermatogonia - which the authors claim on line 89 is a marker of SCs!), along with the detection of markers of various somatic cell populations (albeit at lower levels). This admixture problem influences the results - the authors show ATAC-seq accessibility traces for several genes in Fig. 2E (exhibiting differences between P15 and Adult), including *Ihh*, which is not expressed by spermatogenic cells, and *Col6a1*, which is expressed by peritubular myoid cells. Thus, the methods in this paper are fundamentally flawed, which precludes drawing any firm conclusions from the data about changes in chromatin accessibility among spermatogonia (SCs?) across postnatal testis development. In addition, there already are numerous scRNA-seq datasets from mouse spermatogenic cells at the same developmental stages in question. Moreover, several groups have used bulk ATAC-seq to profile enriched populations of spermatogonia, including from synchronized spermatogenesis which reflects a high degree of purity (see Maezawa et al., 2018 PMID: 29126117 and Schlieff et al., 2023 PMID: 36983846 and in cultured spermatogonia - Suen et al., 2022 PMID: 36509798) - so this topic has already begun to be examined. None of these papers was cited, so it appears the authors were unaware of this work. The authors' methodological choice is even more surprising given the wealth of single-cell evidence in the literature since 2018 demonstrating the exceptional heterogeneity among spermatogonia at these developmental stages (the authors DID cite some of these papers, so they are aware). Indeed, it is currently possible to perform concurrent scATAC-seq and scRNA-seq (10x Genomics Multiome), which would have made these data quite useful and robust. As it stands, given the lack of novelty and critical methodological flaws, readers should be cautioned that there is little new information to be learned about spermatogenesis from this study, and in fact, the data in Figures 2-5 may lead readers astray because they do not reflect the biology of any one type of male germ cell. Indeed, not only do these data not add to our understanding of spermatogonial development, but they are damaging to the field if their source and identity are properly understood. Here are some specific examples of the problems with these data:

1. Fig. 2D - *Gata4* and *Lhcgr* are not expressed by germ cells in the testis.
2. Fig. 3A - *WT1* is expressed by Sertoli cells, so the change in accessibility of regions containing a *WT1* motif suggests differential contamination with Sertoli cells. Since *Wt1*

mRNA was differentially high in P15 (Fig. 3B) - this seems to be the most likely explanation for the results. How was this excluded?

3. Fig. 3D - Since *Dmrt1* is expressed by Sertoli cells, the "downregulation" likely represents a reduction in Sertoli cell contamination in the adult, like the point above. Did the authors consider this?

Reviewer #3 (Public Review):

In this study, Lazar-Contes and colleagues aimed to determine whether chromatin accessibility changes in the spermatogonial population during different phases of postnatal mammalian testis development. Because actions of the spermatogonial population set the foundation for continual and robust spermatogenesis and the gene networks regulating their biology are undefined, the goal of the study has merit. To advance knowledge, the authors used mice as a model and isolated spermatogonia from three different postnatal developmental age points using a cell sorting methodology that was based on cell surface markers reported in previous studies and then performed bulk RNA-seq and ATAC-seq. Overall, the technical aspects of the sequencing analyses and computational/bioinformatics seem sound but there are several concerns with the cell population isolated from testes and lack of acknowledgment for previous studies that have also performed ATAC-seq on spermatogonia of mouse and human testes. The limitations, described below, call into question the validity of the interpretations and reduce the potential merit of the findings.

I suggest changing the acronym for spermatogonial cells from SC to SPG for two reasons. First, SPG is the commonly used acronym in the field of mammalian spermatogenesis. Second, SC is commonly used for Sertoli Cells.

The authors should provide a rationale for why they used postnatal day 8 and 15 mice.

The FACS sorting approach used was based on cell surface proteins that are not germline-specific so there were undoubtedly somatic cells in the samples used for both RNA and ATAC sequencing. Thus, it is essential to demonstrate the level of both germ cell and undifferentiated spermatogonial enrichment in the isolated and profiled cell populations. To achieve this, the authors used PLZF as a biomarker of undifferentiated spermatogonia. Although PLZF is indeed expressed by undifferentiated spermatogonia, there have been several studies demonstrating that expression extends into differentiating spermatogonia. In addition, PLZF is not germ-cell specific and single-cell RNA-seq analyses of testicular tissue have revealed that there are somatic cell populations that express *Plzf*, at least at the mRNA level. For these reasons, I suggest that the authors assess the isolated cell populations using a germ-cell specific biomarker such as *DDX4* in combination with PLZF to get a more accurate assessment of the undifferentiated spermatogonial composition. This assessment is essential for the interpretation of the RNA-seq and ATAC-seq data that was generated.

A previous study by the Namekawa lab (PMID: 29126117) performed ATAC-seq on a similar cell population (THY1+ FACS sorted) that was isolated from pre-pubertal mouse testes. It was surprising to not see this study referenced in the current manuscript. In addition, it seems prudent to cross-reference the two ATAC-seq datasets for commonalities and differences. In addition, there are several published studies on scATAC-seq of human spermatogonia that might be of interest to cross-reference with the ATAC-seq data presented in the current study to provide an understanding of translational merit for the findings.

Author Response

Reviewer #1 (Public Review):

Weaknesses: There appears to be a lack of basic knowledge of the process of spermatogenesis. For instance, the statement that "During the first week of postnatal life, a population of SCs continues to proliferate to give rise to undifferentiated Asingle (As), Apaired (Apr) and Aaligned (Aal) cells. The remaining SCs differentiate to form chains of daughter cells that become primary and secondary spermatocytes around postnatal day (PND) 10 to 12." is inaccurate. The Aal cells are the spermatogonial chains, the two are not distinct from one another. In addition, the authors fail to mention spermatogonial stem cells which form the basis for steady-state spermatogenesis. The authors also do not acknowledge the well-known fact that, in the mouse, the first wave of spermatogenesis is distinct from subsequent waves. Finally, the authors do not mention the presence of both undifferentiated spermatogonia (aka - type A) and differentiating spermatogonia (aka - type B). The premise for the study they present appears to be the implication that little is known about the dynamics of chromatin during the development of spermatogonia. However, there are published studies on this topic that have already provided much of the information that is presented in the current manuscript.

We acknowledge the reviewer's criticism about the inaccuracy and incompleteness of some of the statements about spermatogonial cells and spermatogenesis. We will improve the text accordingly in the reviewed manuscript. We will also clarify the premise of the study which was to complement existing datasets on spermatogonial cells by providing parallel transcriptomic and chromatin accessibility maps of high resolution from the same cell populations at early postnatal, late postnatal and adult stages collected from single individuals (for adults). These features make our datasets comprehensive and an important additional resource for people in the community. We will also revise the description of published studies to be more inclusive.

It is not clear which spermatogonial subtype the authors intended to profile with their analyses. On the one hand, they used PLZF to FACS sort cells. This typically enriches for undifferentiated spermatogonia. On the other hand, they report detection in the sorted population of markers such as c-KIT which is a well-known marker of differentiating spermatogonia, and that is in the same population in which ID4, a well-known marker of spermatogonial stem cells, was detected. The authors cite multiple previously published studies of gene expression during spermatogenesis, including studies of gene expression in spermatogonia. It is not at all clear what the authors' data adds to the previously available data on this subject.

The authors analyzed cells recovered at PND 8 and 15 and compared those to cells recovered from the adult testis. The PND 8 and 15 cells would be from the initial wave of spermatogenesis whereas those from the adult testis would represent steady-state spermatogenesis. However, as noted above, there appears to be a lack of awareness of the well-established differences between spermatogenesis occurring at each of these stages.

The reviewer correctly points that our samples contain both undifferentiated spermatogonial stem cells and differentiated spermatogonia, which is expected from the chosen FACS strategy. We clearly mention the fact that our populations are mixed and that our samples are 85-95% PLZF+ enriched. We also acknowledge the possible presence of contaminating cells that may influence the results and data interpretation in the section "Limitations". We believe that this does not diminish the value of the datasets. But to further increase their usefulness and improve their interpretation, we will conduct new analyses and apply computational methods to deconvolute our bulk RNA-seq datasets in silico (PMID: 37528411) using publicly available single-cell RNA-seq datasets. Such analyses shall correct for cell-type heterogeneity

and provide information about the cellular composition of our cell preparations clarifying the representation of undifferentiated and differentiated spermatogonial cells and the possible presence of somatic cells.

In general, the authors present observational data of the sort that is generated by RNA-seq and ATAC-seq analyses, and they speculate on the potential significance of several of these observations. However, they provide no definitive data to support any of their speculations. This further illustrates the fact that this study contributes little if any new information beyond that already available from the numerous previously published RNA-seq and ATAC-seq studies of spermatogenesis. In short, the study described in this manuscript does not advance the field.

We acknowledge that RNA-seq and ATAC-seq datasets like ours are observational and that their interpretation can be speculative. Nevertheless, our datasets represent an additional useful resource for the community because they are comprehensive and high resolution, and can be exploited for instance, for studies in environmental epigenetics and epigenetic inheritance examining the immediate and long-term effects of postnatal exposure and their dynamics. The depth of our RNA sequencing allowed detect transcripts with a high dynamic range, which has been limited with classical RNA sequencing analyses of spermatogonial cells and with single-cell analyses (which have comparatively low coverage). Further, our experimental pipeline is affordable (more than single cell sequencing approaches) and in the case of adults, provides data per animal informing on the intrinsic variability in transcriptional and chromatin regulation across males. These points will be discussed in the revised manuscript.

The phenomenon of epigenetic priming is discussed, but then it seems that there is some expression of surprise that the data demonstrate what this reviewer would argue are examples of that phenomenon. The authors discuss the "modest correspondence between transcription and chromatin accessibility in SCs." Chromatin accessibility is an example of an epigenetic parameter associated with the primed state. The primed state is not fully equivalent to the actively expressing state. It appears that certain histone modifications along with transcription factors are critical to the transition between the primed and actively expressing states (in either direction). The cell types that were investigated in this study are closely related spermatogenic, and predominantly spermatogonial cell types. It is very likely that the differentially expressed loci will be primed in both the early (PND 8 or 15) and adult stages, even though those genes are differentially expressed at those stages. Thus, it is not surprising that there is not a strict concordance between +/- chromatin accessibility and +/- active or elevated expression.

The reviewer is right that a strict concordance between chromatin accessibility and transcription is not necessarily expected. The text of the revised manuscript will be modified accordingly. However, we would like to note that our data strengthen the observations made by others that in cells from the same lineage, the global landscape of chromatin accessibility is more stable than their transcriptional programs over developmental time.

Reviewer #2 (Public Review):

The objective of this study from Lazar-Contes et al. is to examine chromatin accessibility changes in "spermatogonial cells" (SCs) across testis development. Exactly what SCs are, however, remains a mystery. The authors mention in the abstract that SCs are undifferentiated male germ cells and have self-renewal and differentiation activity, which would be true for Spermatogonial STEM Cells (SSCs), a very small subset of total spermatogonia, but then the methods they use to retrieve such cells using antibodies that enrich for undifferentiated spermatogonia encompass both undifferentiated and

differentiating spermatogonia. Data in Fig. 1B prove that most (85-95%) are PLZF+, but PLZF is known to be expressed both by undifferentiated and differentiating (KIT+) spermatogonia (Niederberger et al., 2015; PMID: 25737569). Thus, the bulk RNA-seq and ATAC-seq data arising from these cells constitute the aggregate results comprising the phenotype of a highly heterogeneous mixture of spermatogonia (plus contaminating somatic cells), NOT SSCs. Indeed, Fig. 1C demonstrates this by showing the detection of Kit mRNA (a well-known marker of differentiating spermatogonia - which the authors claim on line 89 is a marker of SSCs!), along with the detection of markers of various somatic cell populations (albeit at lower levels).

The reviewer is correct that our spermatogonial cell populations are mixed and include undifferentiated and differentiated cells, hence the name of spermatogonia (SCs), and probably also contain some somatic cells. We acknowledge that this is a limitation of our isolation approach. To circumvent this limitation, we will conduct in silico deconvolution analysis using publicly available single cell RNA sequencing datasets to obtain information about markers corresponding to undifferentiated and differentiated spermatogonia cells, and somatic cells. These additional analyses will provide information about the cellular composition of the samples and clarify the representation of undifferentiated and differentiated spermatogonial cells and other cells.

This admixture problem influences the results - the authors show ATAC-seq accessibility traces for several genes in Fig. 2E (exhibiting differences between P15 and Adult), including Ihh, which is not expressed by spermatogenic cells, and Col6a1, which is expressed by peritubular myoid cells. Thus, the methods in this paper are fundamentally flawed, which precludes drawing any firm conclusions from the data about changes in chromatin accessibility among spermatogonia (SCs?) across postnatal testis development.

The reviewer raises concern about the lack of correspondence between chromatin accessibility and expression observed for some genes, arguing that this precludes drawing firm conclusions. However, a dissociation between chromatin accessibility and gene expression is normal and expected since chromatin accessibility is only a readout of protein deposition and occupancy e.g. by transcription factors, chromatin regulators, nucleosomes, at specific genomic loci that does not give functional information of whether there is ongoing transcriptional activity or not. A gene that is repressed or poised for expression can still show clear signal of chromatin accessibility at regulatory elements. The dissociation between chromatin accessibility and transcription has been reported in many different cells and conditions (PMID: 36069349, PMID: 33098772) including in spermatogonial cells (PMID: 28985528) and in gonads in different species (PMID: 36323261). Therefore, the dissociation between accessibility and transcription is not a reason to conclude that our data are flawed.

In addition, there already are numerous scRNA-seq datasets from mouse spermatogenic cells at the same developmental stages in question.

This is true but full transcriptomic profiling like ours on cell populations provides different transcriptional information that is deeper and more comprehensive. Our datasets identified >17,000 genes while scRNA-seq typically identifies a few thousands of genes. Our analyses also identified full length transcripts, variants, isoforms and low abundance transcripts. These datasets are therefore a valuable addition to existing scRNA-seq.

Moreover, several groups have used bulk ATAC-seq to profile enriched populations of spermatogonia, including from synchronized spermatogenesis which reflects a high degree of purity (see Maezawa et al., 2018 PMID: 29126117 and Schlieff et al., 2023 PMID: 36983846 and in cultured spermatogonia - Suen et al., 2022 PMID: 36509798) - so this

topic has already begun to be examined. None of these papers was cited, so it appears the authors were unaware of this work.

We apologize for not mentioning these studies in our manuscript, we will do so in the revised version.

The authors' methodological choice is even more surprising given the wealth of single-cell evidence in the literature since 2018 demonstrating the exceptional heterogeneity among spermatogonia at these developmental stages (the authors DID cite some of these papers, so they are aware). Indeed, it is currently possible to perform concurrent scATAC-seq and scRNA-seq (10x Genomics Multiome), which would have made these data quite useful and robust. As it stands, given the lack of novelty and critical methodological flaws, readers should be cautioned that there is little new information to be learned about spermatogenesis from this study, and in fact, the data in Figures 2-5 may lead readers astray because they do not reflect the biology of any one type of male germ cell. Indeed, not only do these data not add to our understanding of spermatogonial development, but they are damaging to the field if their source and identity are properly understood. Here are some specific examples of the problems with these data:

1. Fig. 2D - Gata4 and Lhcgr are not expressed by germ cells in the testis.

1. Fig. 3A - WT1 is expressed by Sertoli cells, so the change in accessibility of regions containing a WT1 motif suggests differential contamination with Sertoli cells. Since Wt1 mRNA was differentially high in P15 (Fig. 3B) - this seems to be the most likely explanation for the results. How was this excluded?

1. Fig. 3D - Since Dmrt1 is expressed by Sertoli cells, the "downregulation" likely represents a reduction in Sertoli cell contamination in the adult, like the point above. Did the authors consider this?

We acknowledge that concurrent scATAC-seq and scRNA-seq analyses have been done by others but our datasets add to these analyses by providing concurrent chromatin and expression analyses at high resolution in spermatogonial populations at 2 postnatal stages and in adulthood and from individual males (for adult cells). This provides a set of information that adds to the current literature. Doing such analyses in single cells is not tractable financially so we offer an economical alternative that delivers high resolution datasets for these different time points. Our analyses were not meant to study spermatogenesis but to provide a thorough and comprehensive profiling of chromatin accessibility and transcription in postnatal and adult spermatogonial cells.

Our data need careful interpretation to avoid any misleading conclusions. Fig. 2D does not show expression but accessibility which does not tell if a particular locus or gene is expressed or not. Thus, candidates like Gata4 and Lhcgr shown in Fig. 2D are simply associated with DARs but this does not mean that they are expressed. Likewise in Fig. 3A, motifs refer to decreased accessibility and not to expression. Fig. 1C indicates that PND15 cells have low to no expression of 3 Sertoli cells markers (Vim, Tspan17 and Rhox), suggesting little contamination by Sertoli cells. The presence of WT1 in PND15 cells will however be examined more carefully and re-analysed by in silico deconvolution methods using single cell datasets for the revised manuscript. In Fig. 3D, differential contamination by Sertoli cells is possible, this will also be examined by deconvolution methods.

Reviewer #3 (Public Review):

In this study, Lazar-Contes and colleagues aimed to determine whether chromatin accessibility changes in the spermatogonial population during different phases of postnatal mammalian testis development. Because actions of the spermatogonial population set the foundation for continual and robust spermatogenesis and the gene networks regulating their biology are undefined, the goal of the study has merit. To advance knowledge, the authors used mice as a model and isolated spermatogonia from three different postnatal developmental age points using a cell sorting methodology that was based on cell surface markers reported in previous studies and then performed bulk RNA-sequencing and ATAC-sequencing. Overall, the technical aspects of the sequencing analyses and computational/bioinformatics seem sound but there are several concerns with the cell population isolated from testes and lack of acknowledgment for previous studies that have also performed ATAC-sequencing on spermatogonia of mouse and human testes. The limitations, described below, call into question the validity of the interpretations and reduce the potential merit of the findings.

I suggest changing the acronym for spermatogonial cells from SC to SPG for two reasons. First, SPG is the commonly used acronym in the field of mammalian spermatogenesis. Second, SC is commonly used for Sertoli Cells.

We thank the reviewer for the suggestion and will rename SCs into SPGs in the revised manuscript.

The authors should provide a rationale for why they used postnatal day 8 and 15 mice.

We will provide a rationale for the use of postnatal 8 and 15 stages in the revised manuscript. Briefly, these stages are interesting to study because early to mid postnatal life is a critical window of development for germ cells during which environmental exposure can have strong and persistent effects. The possibility that changes in germ cells can happen during this period and persist until adulthood is an important area of research linked to disciplines like epigenetic toxicology and epigenetic inheritance.

The FACS sorting approach used was based on cell surface proteins that are not germline-specific so there were undoubtedly somatic cells in the samples used for both RNA and ATAC sequencing. Thus, it is essential to demonstrate the level of both germ cell and undifferentiated spermatogonial enrichment in the isolated and profiled cell populations. To achieve this, the authors used PLZF as a biomarker of undifferentiated spermatogonia. Although PLZF is indeed expressed by undifferentiated spermatogonia, there have been several studies demonstrating that expression extends into differentiating spermatogonia. In addition, PLZF is not germ-cell specific and single-cell RNA-seq analyses of testicular tissue have revealed that there are somatic cell populations that express Plzf, at least at the mRNA level. For these reasons, I suggest that the authors assess the isolated cell populations using a germ-cell specific biomarker such as DDX4 in combination with PLZF to get a more accurate assessment of the undifferentiated spermatogonial composition. This assessment is essential for the interpretation of the RNA-seq and ATAC-seq data that was generated.

The reviewer is right that our cell populations likely contain undifferentiated and differentiated spermatogonial cells and a small percentage of somatic cells including Sertoli cells. As suggested, we examined the expression of the germ-cell marker Ddx4 in our datasets and observed that Ddx4 is highly expressed. It is indeed more highly expressed than the SSC marker Id4 (average log2CPM of 5 vs 8, respectively). We will include this information in the

revised manuscript. Further, the deconvolution analyses that will be conducted are expected to clarify the cellular composition of our cell populations.

A previous study by the Namekawa lab (PMID: 29126117) performed ATAC-seq on a similar cell population (THY1+ FACS sorted) that was isolated from pre-pubertal mouse testes. It was surprising to not see this study referenced in the current manuscript. In addition, it seems prudent to cross-reference the two ATAC-seq datasets for commonalities and differences. In addition, there are several published studies on scATAC-seq of human spermatogonia that might be of interest to cross-reference with the ATAC-seq data presented in the current study to provide an understanding of translational merit for the findings.

We thank the reviewer for pointing out this study as well as other studies in human spermatogonia. We will cross-reference all of them in the revised manuscript.